



Constraining a complex biogeochemical model for CO₂ and N₂O emission simulations from various land uses by model–data fusion

Tobias Houska¹, David Kraus², Ralf Kiese², and Lutz Breuer^{1,3}

¹Institute for Landscape Ecology and Resources Management (ILR), Research Centre for BioSystems, Land Use and Nutrition (iFZ), Justus Liebig University Giessen, 35392 Giessen, Germany

²Institute of Meteorology and Climate Research – Atmospheric Environmental Research (IMK-IFU), 82467 Garmisch-Partenkirchen, Germany

³Centre for International Development and Environmental Research (ZEU), Justus Liebig University Giessen, 35392 Giessen, Germany

Correspondence to: Tobias Houska (tobias.houska@umwelt.uni-giessen.de)

Received: 16 March 2017 – Discussion started: 17 March 2017

Revised: 22 June 2017 – Accepted: 28 June 2017 – Published: 24 July 2017

Abstract. This study presents the results of a combined measurement and modelling strategy to analyse N₂O and CO₂ emissions from adjacent arable land, forest and grassland sites in Hesse, Germany. The measured emissions reveal seasonal patterns and management effects, including fertilizer application, tillage, harvest and grazing. The measured annual N₂O fluxes are 4.5, 0.4 and 0.1 kg N ha⁻¹ a⁻¹, and the CO₂ fluxes are 20.0, 12.2 and 3.0 t C ha⁻¹ a⁻¹ for the arable land, grassland and forest sites, respectively. An innovative model–data fusion concept based on a multi-criteria evaluation (soil moisture at different depths, yield, CO₂ and N₂O emissions) is used to rigorously test the LandscapeDNDC biogeochemical model. The model is run in a Latin-hypercube-based uncertainty analysis framework to constrain model parameter uncertainty and derive behavioural model runs. The results indicate that the model is generally capable of predicting trace gas emissions, as evaluated with RMSE as the objective function. The model shows a reasonable performance in simulating the ecosystem C and N balances. The model–data fusion concept helps to detect remaining model errors, such as missing (e.g. freeze–thaw cycling) or incomplete model processes (e.g. respiration rates after harvest). This concept further elucidates the identification of missing model input sources (e.g. the uptake of N through shallow groundwater on grassland during the vegetation period) and uncertainty in the measured validation data (e.g. forest N₂O emissions in winter months). Guidance is

provided to improve the model structure and field measurements to further advance landscape-scale model predictions.

1 Introduction

Carbon dioxide (CO₂) and nitrous oxide (N₂O) are two prominent greenhouse gases (GHGs) contributing to global warming, the latter having a global warming potential (GWP) 300 times higher than that of CO₂ considering a 100-year time horizon (Myhre et al., 2013). Terrestrial ecosystems play an important role in the global atmospheric budgets of both GHGs (Cole et al., 1997). The global CO₂ emissions from soils are five times higher than anthropogenic (mainly fossil fuel) CO₂ emissions (Raich and Schlesinger, 1992; updated with recent fossil fuel data by Boden et al., 2010), while agricultural land use released over 60 % of the global anthropogenic N₂O emissions in 2005 (IPCC, 2007). In addition to the radiative forcing of both GHGs, N₂O is currently the main driver of stratospheric ozone depletion (Ravishankara et al., 2009), causing increased ultraviolet radiation, which could result in skin cancer and other health problems (Graedel and Crutzen, 1989). While CO₂ is exchanged with the soil (heterotrophic respiration) and vegetation (photosynthesis and autotrophic respiration), N₂O fluxes refer mainly to the nitrification and denitrification processes occurring only in the soil (Butterbach-Bahl et al., 2013).

Emissions of both GHGs are highly variable in space and time and depend on a multitude of different interacting environmental factors, e.g. land use/management, nitrogen/carbon inputs, meteorological conditions and physical and chemical soil properties (Davidson, 1992; Smith et al., 2003). They are largely regulated by plant physiological (Rochette et al., 1999) and microbial processes (Burton et al., 2008). Field measurements of GHG emissions and environmental drivers have paved the way for a basic understanding of observed emissions patterns. Nevertheless, the large number and complexity of the processes involved in the production and consumption of CO₂ and N₂O are still challenges in the reliable quantification of related GHG emissions (Butterbach-Bahl et al., 2013). Various biogeochemical models have been developed in recent years. These models are used for temporal as well as spatial up-scaling of GHG emissions, hypothesis testing of our understanding of processes, and for scenario analyses and the evaluation of efficient mitigation options (Kim et al., 2015; Molina-Herrera et al., 2016). These include BASFOR (Oijen et al., 2005), CERES-EGC (Gabrielle et al., 2006), COUP (Jansson, 2012), DAYCENT (Parton et al., 1998) and DNDC and its descendant LandscapeDNDC (Haas et al., 2013). However, models are still simplifications of the real world and are prone to multiple sources of uncertainty, i.e. defective model structure and/or parameterization and the current model state (Vrugt, 2016). During model application, poor-quality model forcing data result in further uncertainties about the predicted model outcome (Kavetski et al., 2006). However, there is still no method available to properly address these sources of uncertainty at the same time (Vrugt, 2016). One promising way to reduce the magnitude of uncertainties in model output is to use model–data fusion techniques, i.e. matching model prediction with multiple observations by varying model parameters or states using statistical uncertainty estimation (Keenan et al., 2011). There are several statistical uncertainty estimation methods available, e.g. formal Bayesian approaches such as DREAM (Vrugt, 2016) and informal Bayesian approaches such as GLUE (Beven and Binley, 1992). However, these approaches are mostly used to fit models to single types of observations (Giltrap et al., 2010). Innovative multiple observation data evaluations with model–data fusion are becoming common in ecosystem carbon modelling (Wang et al., 2009) and are more and more important in the nitrogen modelling community (Wang and Chen, 2012). The knowledge gained can and should be used to guide further model improvements (Vrugt, 2016).

This work focuses on establishing model–data fusion in the biogeochemical community – i.e. showing the capability of this technique to improve process understanding through the application of process-based models. We present weekly measurements of CO₂ and N₂O emissions from a developed landscape with different land uses, i.e. arable land, grassland and forest ecosystems, covering a 2-year period of observations. In addition to field measurements, we set up the bio-

geochemical LandscapeDNDC model for each of the three land uses. During model–data fusion with GLUE, we rigorously accept only model runs that return concurrent, acceptable outputs for N₂O, CO₂ and soil moisture at different depths and yields. Posterior model runs are not only evaluated as to whether they fulfil appropriate objective functions but also regarding realistic simulations of GHG emissions for separate seasons, annual sums as well as before and after land management. The model is finally used to estimate the magnitude and uncertainty of C and N fluxes, such as N₂ emissions or autotrophic and heterotrophic CO₂ emissions, which are not yet experimentally quantifiable in situ. The remaining model and data errors are traced back to their potential sources to improve ongoing measurements and future model applications.

2 Materials and methods

2.1 Study area

The study area is located in the catchment of a low mountainous creek (Vollnkirchener Bach) in the municipality of Hüttenberg, Hesse, Germany (50°29′56″ N, 8°33′2″ E). One kilometre north of the village of Vollnkirchen, next to the creek, we established eight transects (oriented mostly vertically to slope) along a valley cross section covering different types of land uses (Fig. 1) for GHG emission measurements. See Table 1 for detailed information on soils characteristics. Three transects (A1–3) are located on arable land to the west of the creek and were cultivated with the same field management and crop rotations (Table 1). Three transects are located in a young European beech (*Fagus sylvatica*) forest (W1–3) with young and old trees on a steep hillside (slope: 10 %) east of the creek. A shallow 0.05 m litter layer characterizes the forest soils. Furthermore, there is one managed and grazed grassland transects (G1) located in the riparian zone at a 4 m distance to the Vollnkirchener Bach. The G1 transect is mainly covered with brown knapweed (*Centaurea jacea*), meadow foxtail (*Alopecurus pratensis*), red clover (*Trifolium pratense*) and ribwort plantain (*Plantago lanceolata*). The groundwater table is close to the surface on the grassland sites. The mean annual wet depositions of nitrate and ammonium were measured for 2013–2015 with 2.70 and 4.32 kg N ha⁻¹ a⁻¹, respectively. Dry deposition of N was not measured and can be assumed to add another 30–60 % to total atmospheric N deposition (Flechard et al., 2011).

In the catchment, the mean annual precipitation is 588 mm, and the mean annual temperature is 10.5 °C for the hydrological year 1 November 2013–31 October 2014 (Seifert et al., 2016). The soil moisture is measured at A3 [0.2, 0.4 and 0.6 m], close to G1 [0.1 and 0.25 m] and at W1 [0.15 and 0.25 m] and has been recorded at an hourly resolution since 2013.

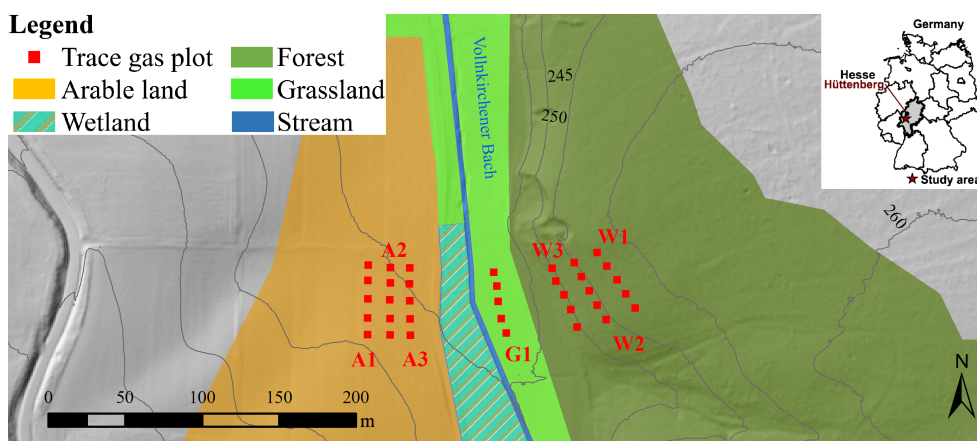


Figure 1. Map of the study area. Red squares represent GHG chamber positions at the different transects. Dark grey contour lines represent 5 m differences in elevation. Light grey areas are outside of the catchment area.

The weekly trace gas measurements began in November 2013 and range so far until December 2015. GHG exchange fluxes were measured manually with non-steady-state opaque chambers, each covering a basal area of 0.12 m². Chambers were placed on frames (both polypropylene), which were inserted approx. 8 cm into the soil in order to facilitate gas-tight sampling as well as to avoid soil structural damage and lateral trace gas leakage. Each chamber is equipped with an extraction septum, a counterbalance valve (in-box pressure balance) and a small fan/ventilator for homogeneous mixing of the headspace air. During a 40 min closure period, five air samples are taken from the chamber headspace at regular time intervals t_0 – t_4 of 10 minutes (0, 10, 20, 30 and 40 min). Samples are analysed by gas chromatography (GC 8610C, SRI Instruments, Torrance, US) with an ECD for N₂O and a methanizer and flame ionization detector for CO₂. Sampling was performed on a weekly basis, with five replicated chambers per transect sampled by the gas sample pooling technique (Arias-Navarro et al., 2013). According to this approach, at any time interval (t_0 – t_4), 10 mL headspace samples are collected subsequently from any of the five replicated chambers and are pooled into one gas-tight glass vial (SRI Instruments). The trace gas fluxes are calculated from the rate of change in the headspace gas concentration over time by linear regression and were corrected for the chamber temperature, atmospheric pressure and chamber volume according to Barton et al. (2008). All measurements with a regression quality of $r^2 < 0.7$ for CO₂ (using at least four individual samples) were rejected.

Soil emissions of CO₂ and N₂O can be subject to significant diurnal patterns, with peak values observed in the early afternoon (Savage et al., 2014), impeding the up-scaling of hourly measured emissions (usually obtained at midday) to daily values. We performed multiple linear regression (ordinary least squares regression including air temperature, relative humidity and water-filled pores space) to account

for the difference between, for example, daytime (Wohlfahrt et al., 2005a) and night-time respiration (Wohlfahrt et al., 2005b). In our dataset, only CO₂ emissions showed significant correlations with the mentioned environmental drivers on arable land ($r^2 = 0.53$), grassland ($r^2 = 0.59$) and forest ($r^2 = 0.51$). Following Subke et al. (2003), we derived an hourly integration formula in order to obtain daily representative mean values of CO₂ emissions from our field measurements conducted mostly between 09:00 and 17:00. N₂O emissions are up-scaled to daily mean values with the common approach, i.e. by multiplying hourly emissions by 24. Annual CO₂ and N₂O emissions are calculated by linear interpolation between the measurements. All the underlying data in Sect. 2.1 and 2.2 are available upon request from a database (<http://fb09-pasig.umwelt.uni-giessen.de:8081/>).

2.2 Modelling approach

2.2.1 Model set-up

We tested the biogeochemical model framework LandscapeDNDC (Haas et al., 2013) with the observed data from our study area. Individual models were set up for arable land, grassland and forest ecosystems. The models describe different processes in ecosystem compartments, i.e. mathematical descriptions of microclimate, water cycle, plant physiology and soil biogeochemical processes. We applied the biogeochemical model MeTr^x (Kraus et al., 2015) and the water cycle model watercycleDNDC (Kiese et al., 2011) for all land uses. The biogeochemical model MeTr^x simulates the turnover of soil organic matter and plant debris depending on their chemical structures (e.g. lignin and cellulose content, C/N ratio), soil properties (e.g. pH value) and meteorological drivers. Following the “anaerobic balloon” concept of Li et al. (2000), major metabolites (e.g. NO₃) are distinguished between aerobic and anaerobic counterparts in order to simulate the share of nitrification and denitrification and

the related production of GHG emissions. Simulated model outputs are, among others, emissions of CO₂ and N₂O. There exists an effect of the simulated gaseous losses on the available nutrition for plant growth, which in turn affects water cycle through changing water uptake and transpiration. However, we neglect this comparably minor interaction effect in our model–data fusion approach, as outlined in Sect. 2.3.2. The watercycleDNDC model simulates soil water dynamics, i.e. potential evapotranspiration based on Thornthwaite and Mather (1957), transpiration depending on gross primary productivity, the water use efficiency of the modelled plant types and soil water flow based on a cascading bucket model approach (Kiese et al., 2011). The latter determines the advective transport of nutrients into deeper soil layers.

All models refer to a one-dimensional soil column, i.e. assuming homogeneous conditions in lateral directions, and were run with a daily time step resolution. Table 1 provides an overview of the major model driving data, i.e. meteorological data and land use-specific soil and vegetation characteristics. To simulate plant growth on the three different land use types, we selected the individual physiology modules arableDNDC, grasslandDNDC (Kim et al., 2015; Molina-Herrera et al., 2016) and PSIM (Grote et al., 2009).

Arable soils are Stagnic Luvisols with a thick loess layer, modelled down to 2.0 m with 80 layers, while the actual soil depth is unknown. Gleysols in the meadow grassland site were modelled down to 0.5 m (set-up with 40 layers), corresponding to the mean annual groundwater table depth. The thin and stony soil at the forest site is a cambisol and modelled down to bedrock (0.55 m, set-up with 45 layers) with a litter height of 0.05 m. The bulk density increases with depth for every land use, while soil organic carbon and nitrogen decrease with depth. We run simulations for all land uses at a daily time resolution for 6 years, starting on 1 January 2010, using the data from Table 1 as initialization and using a model spin-up time of 2 years.

2.2.2 Model–data fusion

For the multi-objective Bayesian model calibration, we used a two-tiered Generalized Likelihood Uncertainty Estimation (GLUE) approach (Beven and Binley, 1992). Tier I is designed to constrain the investigated parameter space for simulating water cycle and plant growth, while tier II builds on tier I and aims to fit the parameters for the biogeochemical process which drives the GHG emissions. The model was iterated in both tiers 100 000 times by changing the parameter sets using Latin hypercube sampling with the Python software SPOTPY (Houska et al., 2015). The parameters for the physiology and the water-cycle modules were treated as land-use specific, while the parameters of the biogeochemical model were calibrated using the data from all land uses (Table A1 in Appendix). We presuppose no prior knowledge besides the given parameter ranges, i.e. we assume a uniform (non-informative) prior probability distribu-

tion for all parameters. We statistically judged the performance of every parameter set to reproduce measurements with a root mean squared error (RMSE). Similar to Bloom and Williams (2015), we do not explicitly consider measurement uncertainty during the model–data fusion. As shown in Houska et al. (2017), one-tier GLUE-based multi-objective model calibration can result in very low acceptance rates, down to 0.01 %. We therefore considered a two-tier GLUE approach in order to increase the identifiability and accuracy of the accepted model runs.

Tier I In the first step, we constrained the parameter space of the hydrology and plant physiology modules of LandscapeDNDC by investigating the respective parameters of both models (Table A1). We accepted only model runs that were within the best 5 % of all simulated RMSEs in terms of the respective variable – WFPS at different depths (arable land at 0.2, 0.4 and 0.6 m, grassland at 0.1 and 0.25 m and forest at 0.15 and 0.25 m), as well as yield on arable land. Parameter sets were accepted if they belonged to the 5 % best model runs for each land use. That is, we took the best 5 % of the RMSEs for each respective output variable and took only the intersecting parameter set, which are all from the selected variables for one land use. The results of tier I are summarized in Figs. A1–A4 in the Appendix and are not further discussed in this study, as they belong to the initialization of the model.

Tier II To achieve realistic GHG simulations from the MeTr^x biogeochemical module of LandscapeDNDC, we took the posterior parameter boundaries of tier I and ran GLUE with all parameters of Table A1 again. This time, we considered the best 5 % of all RMSEs in terms of the respective N₂O and CO₂ emissions for each land use (A1–3, G1 and W1–3). Again, only the 5 % best intersecting parameter sets were accepted per land use. These results are shown in the following chapters. There was no major effect of the biogeochemical model parameters on the WFPS simulation, i.e. simulated soil moisture did not change substantially with changing biogeochemical model parameters.

Posterior model runs of tier II were further investigated in three different ways:

1. Seasonal comparisons of measured and modelled emissions for spring (21 March–20 June), summer (21 June–20 September), autumn (21 September–20 December), and winter (21 December–20 March).
2. Management comparison of measured and modelled emissions, i.e. investigation of model performance within 2 weeks before and 2 weeks after management events to check implemented routines in generating hot moments, e.g. after fertilizer application.

Table 1. Input settings of the LandscapeDNDC model for the three different land uses in the Vollnkirchener study region, based on measurements and farmers' management documentation. When spans are given, they reflect observed ranges for measurements used throughout the set-up of the soil profile, given from the top layer setting to the bottom layer. The soil depth was estimated for model set-up; F, fertilizer application; M, manure application.

Input	Arable (A1–3)			Grassland (G1)		Forest (W1–3)	Unit
Vegetation type	Sep 10–Jul 11	Winter barley		Perennial grass		Light beech forest	–
	Aug 11–Aug 12	Rape					
	Oct 12–Aug 13	Winter wheat					
	Oct 13–Aug 14	<i>Triticale</i>					
	Sep 14–Aug 15	<i>Triticale</i>					
	Oct 15–Jul 16	Rape					
Management	2 Mar 12	166.5 kg N ha ⁻¹	(F)	1 Feb 13	Grazing		–
	2 Apr 12	49.9 kg N ha ⁻¹	(F)	1 May 13	Harvest		
	8 Nov 12	56.2 kg N ha ⁻¹	(F)	1 Sep 13	Grazing		
	11 Mar 13	54.0 kg N ha ⁻¹	(F)	2 Mar 14	Grazing		
	23 Apr 13	53.8 kg N ha ⁻¹	(F)	1 May 14	Harvest		
	3 May 13	29.3 kg N ha ⁻¹	(M)	1 Sep 14	Grazing		
	3 May 13	538.0 kg C ha ⁻¹	(M)	20 Jan 15	Grazing		
	12 Nov 13	29.0 kg N ha ⁻¹		29 Jun 15	Harvest		
	12 Nov 13	533.0 kg C ha ⁻¹	(M)	26 Sep 15	Grazing		
	11 Mar 14	54.0 kg N ha ⁻¹	(F)				
	1 Apr 14	53.8 kg N ha ⁻¹	(F)				
	8 May 14	40.5 kg N ha ⁻¹	(F)				
	22 Sep 14	149.0 kg C ha ⁻¹	(M)				
	22 Sep 14	8.1 kg N ha ⁻¹	(M)				
	8 Nov 14	1032.0 kg C ha ⁻¹	(M)				
	8 Nov 14	56.2 kg N ha ⁻¹	(M)				
	11 Mar 15	1564.0 kg C ha ⁻¹	(M)				
	11 Mar 15	85.1 kg N ha ⁻¹	(M)				
	10 Apr 15	59.4 kg N ha ⁻¹	(F)				
	30 Aug 15	59.4 kg N ha ⁻¹	(F)				
12 Nov 15	29.0 kg N ha ⁻¹	(M)					
12 Nov 15	532.0 kg C ha ⁻¹	(M)					
Soil texture	Sandy clay loam			Sandy clay loam	Sandy clay loam	–	
Soil type	Stagnic Luvisol			Gleysol	Cambisol		
Bulk density	1.55–1.60			1.20–1.44	1.36–1.49	g cm ⁻³	
Organic carbon	1.57–0.91			2.55–0.71	3.61–1.73	%	
Total soil nitrogen	0.16–0.09			0.29–0.08	0.21–0.11	%	
Clay content	23–26			24–25	24–26	%	
pH	6.45			4.42	3.5–5.5	–	
Soil depth	2.00			0.50	0.55	m	

3. Model performance in simulating magnitude and uncertainty of C and N fluxes not measured in situ, such as N₂ or autotrophic and heterotrophic components of CO₂ emissions.

3 Results and discussion

3.1 Measured N₂O fluxes

To determine the representativeness of each transect for a given land use, the respective differences in measured N₂O emissions were compared (Table 2). The temporal dynamics

of N₂O emissions are presented (Fig. 2), distinguishing between different seasons (Fig. 3) and before/after management events (Fig. 4).

Arable land N₂O fluxes: emissions on arable land vary between 0 and 0.3 kg N₂O–N ha⁻¹ day⁻¹. There were no significant differences over time between the three weekly measured transects on arable land (Table 2). The highest emissions occur mostly after management events. Mineral fertilizer application in particular stimulates N₂O emissions, causing hot moments from, for example, March to May 2014. The input of N through manure application has a minor influence on the magnitude of N₂O emissions. The mean annual measured N₂O emissions from arable land are comparably high with 4.5 kg N₂O–N ha⁻¹ a⁻¹ (Jungkunst et al., 2006), equalling a GWP of 575 kg CO₂–C equiv. ha⁻¹ a⁻¹. With a yearly fertilizer application of 192.9 kg N a⁻¹ a mean annual emission factor (EF) of 2.3 % (varying between 2.0 % for A2 and 2.9 % for A3) can be calculated, where 1 kg N ha⁻¹ a⁻¹ is attributed to the background emissions of unfertilized soil (IPCC, 1997). This EF is outside the IPCC-assumed range of 1.25 ± 1 % and over the average EF (1.56 %) of several (*n* = 56) agricultural sites in Germany (Jungkunst et al., 2006). A robust finding throughout the literature is that reduced nitrogen input would lead to lower emissions and therefore more climate-friendly agriculture (Bouwman et al., 2002).

Grassland N₂O fluxes: emissions from the grazed grassland vary between –0.0019 and 0.014 kg N ha⁻¹ day⁻¹. High emissions were measured after grazing, e.g. in March 2014 when sheep dung was stimulating N₂O emissions. Negative values depict N₂O uptake and are frequently found under prevailing wet conditions in spring, a finding that was also reported by Glatzel and Stahr (2001). The grassland annual N₂O emissions are much lower than those observed for the arable system (A1–3). However, with 0.29 kg N₂O–N ha⁻¹ a⁻¹ are they in accordance with a study site 12 km northeast of our site, where annual emissions range from 0.18 to 0.79 kg N₂O–N ha⁻¹ a⁻¹ on an unfertilized grassland with shallow groundwater table (Kammann et al., 1998). Their study also reports a similar seasonal pattern to our measurements, with emissions close to zero in the dry and colder autumn months. The measured annual emissions are below the assumed background level of N₂O–N emissions of 1 kg N₂O–N ha⁻¹ a⁻¹ from agricultural soils (IPCC, 1997). The annual N₂O emissions are equal to a GWP of 37 kg CO₂–C equiv. ha⁻¹ a⁻¹. The EF through grazing is 3.8 %, which is in accordance with typical emissions factors from extensive grazed grasslands, ranging globally from 0.2 to 9.9 % (Oenema et al., 1997).

Forest N₂O fluxes: significant differences were found for the forest transects W2 and W3, which can be explained by natural variations along the steep hillslope – on the hillside (W2) the soil is potentially washed out through lateral transport, leading to decreased nutrient availability, compared to the drier top (W1, +200 % N₂O emissions) and the wetter hillfoot (W3, +330 % N₂O emissions). The N₂O emis-

sions from the forest transects are mostly low, ranging between –0.003 and 0.004 kg N ha⁻¹ day⁻¹. Higher emissions were measured only for several weeks in January 2014, with the highest values observed at W1. We attribute this to freeze–thaw effects, typically found when year-around measurements are considered (Papen and Butterbach-Bahl, 1999). Negative fluxes were measured, for example in March and May 2014. The underlying process of N₂O uptake has been reported before (e.g. Flechard et al., 2005; Neftel et al., 2007) and is assumed to be a microbial process, in which denitrifiers use N₂O as an electron acceptor for respiration under wet/anaerobic conditions (Bremner, 1997). Negative emissions occur during times with high WFPS (Fig. A3), which is in accordance with Bremner (1997). However, our measured negative emissions are low compared to the variance between transects (W1–3), i.e. they could also originate from measurement errors. Our annual measured emissions in forests are 0.08 kg N₂O–N ha⁻¹ a⁻¹ (GWP of 10 kg CO₂–C equiv. ha⁻¹ a⁻¹ CO₂ emissions), which is much lower than that at adjacent grassland and arable sites. Moreover, this value is almost 2 orders of magnitude lower than the N₂O emissions (5.1 kg N₂O–N ha⁻¹ a⁻¹) measured from a beech forest in Högelwald, Germany (Papen and Butterbach-Bahl, 1999). A likely reason is the substantially higher annual deposition rate of 25 kg N ha⁻¹ a⁻¹, an N input five times higher than that in our system. However, our measurements of N deposition only include wet deposition. Additional dry depositions are often assumed to add another 30–60 % to total atmospheric N deposition (Flechard et al., 2011).

3.2 Measured CO₂ fluxes

Emissions measured using our closed chamber on arable land and grassland include those from soil and vegetation, as entire plants are covered by the chamber. Therefore, we interpret these emissions as total ecosystem respiration (TER). In contrast, chambers in the forest were placed on the forest floor without any vegetation inside; thus, these measurements include soil (heterotrophic) and root (autotrophic) respiration, i.e. belowground respiration only. To determine the representativeness of each transect for a given land use, the respective differences in measured CO₂ emissions were compared to each other (Table 3). The measured CO₂ emissions are given over time (Fig. 5), separated into different seasons (Fig. 6) and before/after management events occur (Fig. 7).

Arable TER: measured values from our arable transects range up to 175.2, 199.6 and 143.1 kg C–CO₂ ha⁻¹ day⁻¹ for A1, A2 and A3 respectively and are not significantly different between the transects (compare Table 3). Emissions occur mainly during the growing season, starting in March and ending in November. For a comparable study site in southern Finland, reported daily TER values under barley were between 23.6 to 235.6 kg C–CO₂ ha⁻¹ day⁻¹ during May and September (Lohila et al., 2003), which is in the same range as our observations. The annual sum of our TER

Table 2. Mean measured annual fluxes (November 2013–December 2015) on the different land use transects of the Vollnkrichener Bach study area. Differences between the investigated transects and land uses for measured and modelled N₂O emissions in kg N–N₂O ha⁻¹ a⁻¹.

	A1	A2	A3	G1	W1	W2	Measured	Mean measured	Mean simulated	Posterior RMSE
A1							4.08			0.0326–0.0353
A2							3.87	4.49	7.33	0.0238–0.0278
A3							5.53			0.0285–0.0329
G1	*	*	*				0.29	0.29	0.69	0.0029–0.0038
W1	*	*	*				0.09			0.0022–0.0025
W2	*	*	*	*			0.03	0.08	0.33	0.0014–0.0021
W3	*	*	*			*	0.13			0.0018–0.0021

* Significant difference ($p < 0.05$, Kruskal–Wallis test). Arable (A1–3), grassland (G1), wetland (G2), forest (W1–3), RMSE in kg N–N₂O ha⁻¹ day⁻¹.

emissions is 19.96 ± 2.36 t C–CO₂ ha⁻¹ a⁻¹. This is slightly lower than yearly TER measured on a winter wheat study site in Belgium with 23.18 t C–CO₂ ha⁻¹ a⁻¹ (Suleau et al., 2011). Demyan et al. (2016) reported lower values, with an average total of 11.43 t C–CO₂ ha⁻¹ a⁻¹, derived from observations spanning six growing seasons in southwestern Germany. However, all studies are possibly prone to overestimations of the emissions from September to November, as daily emissions are generated with a multiple linear regression model, and in our case, are based on our hourly measurements of air temperature and soil moisture. Such methods do not fully account for management effects, such as harvests (Subke et al., 2003).

Grassland TER: emissions are close to zero in the winter months (December to February) and highest during the growing season. A distinct negative correlation between the measured TER with WFPS was found during wet conditions from end of June to July in 2014. In this time, emissions decrease to 41.0 kg C–CO₂ ha⁻¹ day⁻¹. The total yearly emissions are 11.79 t C–CO₂ ha⁻¹ a⁻¹, which agrees well with the mean yearly emissions reported for 19 different grassland sites across Europe, with mean annual emissions of 12.83 t C–CO₂ ha⁻¹ a⁻¹ (Gilmanov et al., 2007). However, due to the many different grassland sites considered in their study, Gilmanov et al. report a much wider range of observed annual TER values, from 4.9 to 16.4 t C–CO₂ ha⁻¹ a⁻¹. They also found that management is a main influencer of TER, where intensively managed grasslands produce higher emissions than extensively managed grasslands. With regard to grazing, we found only a minor direct impact on the measured flux rates (Fig. 7).

Forest belowground respiration: the mean measured belowground respiration spans between minimum values of 2.1 to 4.5 and maximum values of 9.3 to 19.9 kg C–CO₂ ha⁻¹ day⁻¹ between the different transects (W1–3). While we found higher emissions in the summer months, seasonal differences have a lower magnitude of TER on arable and grassland. This was expected, as we do not measure

aboveground biomass respiration on our forest study site. Overall, rewetting has the strongest influence on changes in belowground respiration in our forest study sites. The highest emissions occurred in July 2014 after several rewetting events of the uppermost soil layer (Fig. A1). Xiang et al. (2008) reported that multiple rewetting leads to respiration rates of up to 8 times higher. The total yearly soil emissions are 2.98 ± 0.89 t C–CO₂ ha⁻¹ a⁻¹, which is at the lower end of other European forest ecosystems, e.g. 6.6 ± 2.9 t C–CO₂ ha⁻¹ a⁻¹, as reported by Janssens et al. (2001). The uphill transect W1 has the highest emission rates throughout the year and shows significant differences when compared to W2 and W3. This transect is less shaded by trees, resulting in a 1.3 °C higher annual mean soil temperature compared to W2 and W3, likely causing higher CO₂ emissions (Table 3).

3.3 Modelled N fluxes

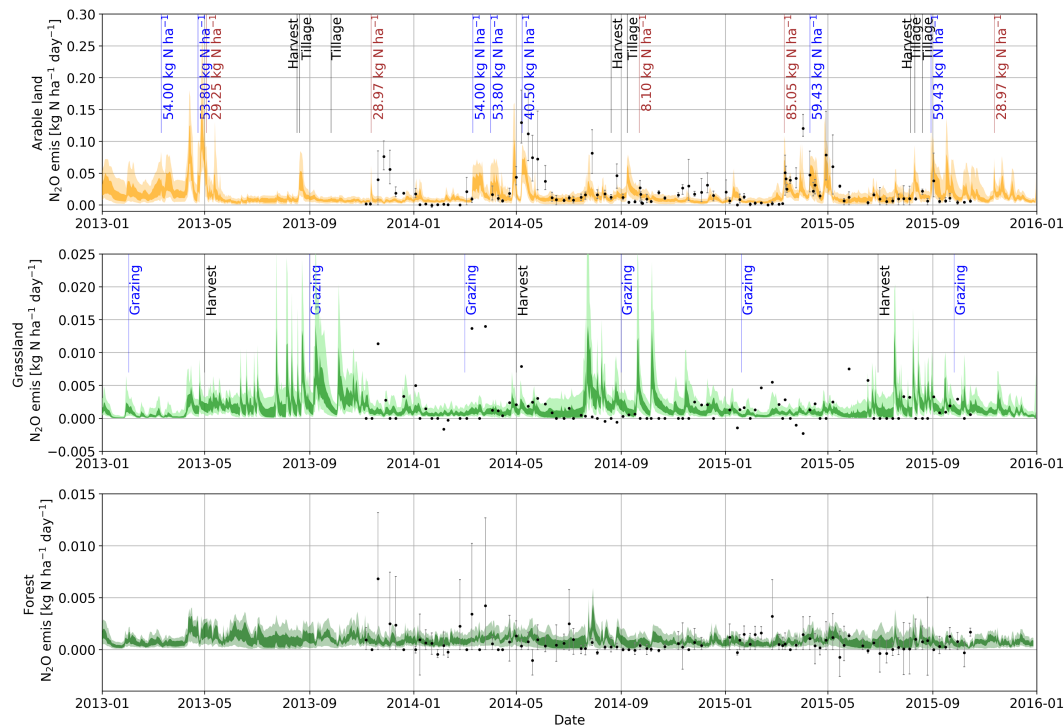
After selecting the posterior model runs as described in Sect. 2.3.2, we found the model to be generally capable of reproducing the measured data and consequently investigated the modelled C and N cycles in more detail. The modelled N₂O emissions are shown for the different land uses over time (Fig. 2), separated into different seasons (Fig. 3) and before/after management events occur (Fig. 4). The complete modelled N cycle is given in Table 4.

Arable land N cycle: the arable land simulations consider an annual N input of 200 kg N ha⁻¹ a⁻¹. This input is balanced by 108.6 ± 50.1 kg N ha⁻¹ a⁻¹ gaseous (primarily N₂), 30.0 ± 29.9 kg N ha⁻¹ a⁻¹ nitrate leaching and 99.7 ± 7.8 kg N ha⁻¹ a⁻¹ harvest losses (Table 4), meaning that the modelled outputs are higher than the given inputs. This gap in the annual N cycle is fed by soil storage in the model, indicating N depletion over time. Even though N losses through NO₃⁻ and particularly N₂O emissions (7.3 ± 2.3 kg N ha⁻¹ a⁻¹) are only a minor proportion of the total N balance, both rates are high regarding their environmental impacts as a GHG contributing to global warm-

Table 3. Mean measured annual fluxes (November 2013–December 2015) from the different land use transects of the Vollnkirchener Bach study area. Differences between the investigated transects and land uses for measured and modelled CO₂ emissions in t C–CO₂ ha⁻¹ a⁻¹.

	A1	A2	A3	G1	W1	W2	Measured	Mean measured	Mean simulated	Posterior RMSE
A1							20.10			30.73–36.38
A2							22.25	19.96	20.53	35.66–42.26
A3							17.54			22.90–28.46
G1							11.79	11.79	13.24	7.01–9.08
W1	*	*	*	*			4.00			3.53–3.89
W2	*	*	*	*	*		2.38	2.98	3.28	3.37–4.07
W3	*	*	*	*	*		2.56			3.15–3.96

* Significant difference ($p < 0.05$, Kruskal–Wallis test). Arable (A1–3), grassland (G1), wetland (G2), forest (W1–3), RMSE in kg C–CO₂ ha⁻¹ day⁻¹.

**Figure 2.** Measured and modelled N₂O emissions from different land use. Measurements are given as grey error bars showing the variance between the replicated transects and the mean value as a black dot. Posterior model uncertainty is given in light colour for the 5th and 95th percentiles and dark colour for the 25th and 75th percentiles. Vertical lines indicate management events. In the uppermost panel, blue coloured vertical bars indicate fertilizer application, while brown colours indicate manure application.

ing and as a water pollutant regarding eutrophication and drinking water supply, respectively. However, the uncertainty related to our estimated NO₃⁻ leaching rate is overall the largest source of uncertainty in our N balance. These estimates cannot be sufficiently constrained with the given observation data, but they are in accordance with other reported N leaching rates on arable land in Germany (Siemens and Kaupenjohann, 2002).

The simulated N₂O emissions contribute 3.1 % to the total simulated N losses. The underlying model runs follow the trend of the observation data. Hot moments can be observed after fertilizer applications, and they are predicted by the model in time but sometimes not in magnitude (e.g. March to May 2014). During these events, soil moisture is often not modelled accurately: the model predicts rewetting processes that have not been measured at the same magnitude (Fig. A1), which might explain the overestimated fluxes. One

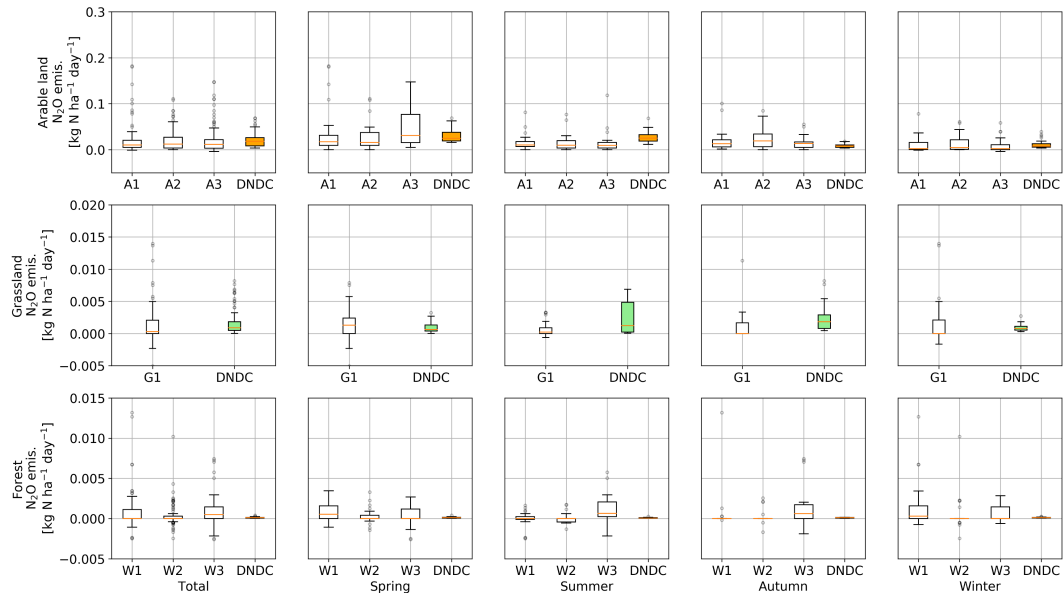


Figure 3. Observed and modelled N₂O emissions for spring (21 March–20 June), summer (21 June–20 September), autumn (21 September–20 December) and winter (21 December–20 March).

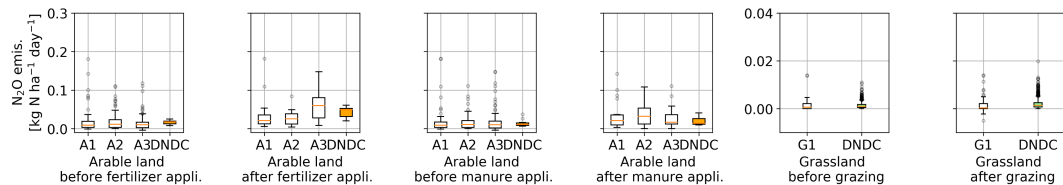


Figure 4. Management effects on N₂O emissions. Measured and modelled emissions within a time window of 2 weeks before and 2 weeks after a management event.

possible reason may also be uncertain rainfall model input data. Kavetski et al. (2006) found the measurements of precipitation within a catchment to be uncertain, as the trajectory of storm cells through a catchment may be different for each storm and may not have their centres at the rain gauge, where rainfall inputs are traditionally measured. Our rainfall data are measured 4 km northeast of the trace gas study area and is likely affected by such uncertainties.

The total simulated and measured emissions on the arable site are highest in the spring (Fig. 3). While the transects A1 and A2 vary, with 95 % of the values between 0 and 0.05 kg N₂O–N ha⁻¹ day⁻¹, A3 shows more variation, up to 0.15 kg N₂O–N ha⁻¹ day⁻¹. As A3 is located at the hill toe, we attribute this effect to the lateral transport of nitrate from uphill. However, our one-dimensional model setup does not cover lateral water and nutrient transport; accordingly, the model is not able to predict the higher emissions at A3 in the spring. While such a process is part of complex integrated hydro-biogeochemical catchment models (Haas et al., 2013; Klatt et al., 2017; Wlotzka et al., 2013), it has not yet been confirmed experimentally. The distributions of the measured emissions in the summer, autumn and winter seasons

are well in accordance with the modelled emissions. Furthermore, the modelled emissions are also in agreement with emissions measured before and after manure applications (Fig. 4). This result agrees with a study by Molina-Herrera et al. (2016) who found LandscapeDNDC to be capable of simulating agricultural N₂O emissions. However, in our case, the model overestimates peak emissions before fertilizer applications, which leads to higher mean annual modelled emissions (7.33 kg N₂O–N ha⁻¹ a⁻¹). This is 2.8 kg N₂O–N ha⁻¹ a⁻¹ higher than our observed emissions and is even outside the large model uncertainty of 2.3 kg N₂O–N ha⁻¹ a⁻¹. Hence, future research should specifically investigate the reason for this overestimation of peaks, either by revising the model structure or by identifying other sources of model uncertainty.

Grassland N cycle: grassland simulations consider an annual N input of 14.6 kg, with 7.6 kg coming from modelled biomass that is transferred into dung and urine applied by grazing sheep. The simulated N loss is substantially larger than the N input, with 22.3 ± 13.3 kg N ha⁻¹ a⁻¹ gaseous losses (primarily N₂), 1.5 ± 3.19 kg N ha⁻¹ a⁻¹ occurring as nitrate leaching and 29.8 ± 9.4 kg N ha⁻¹ a⁻¹ as biomass

removal through grazing sheep and harvest (hay making). Comparing inputs and outputs, we simulated a mean nitrogen gap of $38.9 \pm 25.9 \text{ kg N ha}^{-1} \text{ a}^{-1}$. The model suggests decreasing soil organic N stocks. So far, we have only initial measurements of soil organic N content. However, we assume that the source of additional N in the form of nitrate in shallow groundwater is a potential dominating process that is not included in the current LandscapeDNDC version we used. Liebermann et al. (2017) used a revised LandscapeDNDC setup for hypothesis testing to identify potential additional N sources in groundwater-dominated grasslands and showed that groundwater N uptake is a likely contributor.

Taking a closer look at the modelled N₂O emissions, one can see that the model did not reproduce high or negative (N₂O uptake) emissions. Currently, LandscapeDNDC does not consider any N₂O uptake, and accordingly, negative fluxes cannot be simulated by the model. The peaky dynamics of the simulated N₂O emissions, especially from August 2014 to January 2015, are not confirmed by the measurements, indicating possible measurement errors during this period of time. In a grazed system with, in our case, approximately 70 sheep per hectare, the animal urine patches create emissions hot spots. With only five chambers, it is possible that the measurements could miss these hot spots. Additionally, the LandscapeDNDC model will assume that the manure is uniformly spread over the field, producing emissions that are likely to be higher than those from non-urine patches, but lower than those from urine patches. One has also to consider the temporal mismatch of our weekly N₂O measurements and the hourly simulations, making a full match of the observations with the simulations difficult. So far, there is no clear effect of grazing on the N₂O emissions on the grassland site in both the measurements and modelled results (Fig. 4). The mean modelled annual emissions overestimate the observations by $0.4 \text{ kg N}_2\text{O-N ha}^{-1} \text{ a}^{-1}$, and even the simulated uncertainty bounds of $0.27 \text{ kg N}_2\text{O-N ha}^{-1} \text{ a}^{-1}$ do not capture the measured dynamics.

Forest N cycle: the N input is given for the forest model only considering atmospheric deposition with an annual amount of $7.0 \text{ kg N ha}^{-1} \text{ a}^{-1}$. Gaseous losses amount to $1.8 \pm 2.0 \text{ kg N ha}^{-1} \text{ a}^{-1}$. Leaching contributes to 2.0 % of the N output. The rest ($3.3 \pm 2.0 \text{ kg N ha}^{-1} \text{ a}^{-1}$) is allocated into biomass and soil. By taking a closer look at the N₂O emissions (Fig. 2), we see that the model fails to reproduce the observed emission dynamics. The observed N₂O emissions have high error bars, and not all transects are driven by frost–thaw cycles or N₂O uptake at the same time (Table 2). Parameterizing and simulating the forest transects independently from each other would improve the simulations. One limiting factor is that both N₂O uptake and frost–thaw cycles are not included in the current version of LandscapeDNDC. We therefore recommend the inclusion of frost–thaw cycles (e.g. based on De Bruijn et al., 2009) in the model, as this process can have a major influence on N₂O inventories, e.g. up to 73 % of the total annual

N₂O loss at a forest site in Högelwald, Germany (Papen and Butterbach-Bahl, 1999). The mean modelled annual emissions ($0.33 \pm 0.15 \text{ kg N ha}^{-1} \text{ a}^{-1}$) overestimate the observed emissions on all transects.

3.4 Modelled C fluxes

The modelled CO₂ emissions are shown for the different land uses over time (Fig. 5), separated into different seasons (Fig. 6) and before/after management events (Fig. 7). The complete modelled C cycle is given in Table 5.

Arable land C cycle: the LandscapeDNDC simulations for the arable system predict a mean annual gross carbon uptake of $25.7 \pm 1.3 \text{ t C-CO}_2 \text{ ha}^{-1} \text{ a}^{-1}$. $20.5 \pm 1.8 \text{ t C-CO}_2 \text{ ha}^{-1} \text{ a}^{-1}$ leaves the system through respiration, to which maintenance respiration contributes the largest proportion (65 %). This is in accordance with annual measured losses (Table 3). The harvest output is with $4.7 \pm 0.4 \text{ t C ha}^{-1} \text{ a}^{-1}$ and is in good agreement with the observed yields (Fig. A4). However, the temporal dynamics of the modelled TER on the arable land study site underestimate the emissions in the summer season (Fig. 6), and the mean modelled fluxes are substantially lower than those measured before and after the harvest (Fig. 7).

Tillage and harvest events occur in the summer season. While the observed emissions drop after harvest by 25 %, the modelled emissions drop by 50 %. The reason for this is either an underestimation of the emissions through LandscapeDNDC (after harvest events until tillage occurs) or uncertainties in the measured CO₂ emissions upscaling method (discussed in Sect. 2.1). As microbial processes can oxidize more soil carbon after harvests (resulting in higher heterotrophic respiration), we assume that the discrepancy stems from the model simulations. There are studies, e.g. Buyanovsky et al. (1986), which report the highest soil respiration rates after harvests. The modelled and measured soil CO₂ emissions agree well after tillage. However, unless there is a gap of 2 weeks or more between harvest and tillage, the “pre-tillage” results will include some post-harvest effects, and the “post-harvest” results will also include some post-tillage effects. Our intention to present the data grouped by these events are the discrepancies between modelled and observed CO₂ dynamics. There is a sharp drop of modelled CO₂ emissions after harvest due to the prompt absence of autotrophic respiration. In reality, there will likely be some ongoing metabolic respiration of plant tissue remaining in the field, which is not represented by the “assumed” dead plant material in the model. After incorporation of harvest residues (at tilling), modelled CO₂ emissions increase again sharply. The sharp increase is due to the incorporation and hence availability of fresh litter (stubble) and a temporary stimulation of decomposition by the model due to the disruption/aeration of the soil structure. Both, overestimation of fresh litter and/or stimulation of decomposition by the model

Table 4. Simulated nitrogen fluxes given by posterior model runs and their uncertainty on different land use in kg N ha⁻¹ a⁻¹. N manure on grassland includes urine and dung input by sheep. Biomass output on grasslands combines harvest export and biomass leaving the system through sheep. Arable land model assumes 20 % return of stubble to field.

Modelled N flux	Arable land	Grassland	Forest
N deposition	7.02	7.02	7.02
N manure	57.55	7.57	0
N fertilizer	135.37	0	0
Total input	199.94	14.59	7.02
NO emis.	0.57 ± 0.16	0.46 ± 0.21	0.45 ± 0.33
N ₂ emis.	62.55 ± 26.83	18.69 ± 10.91	1 ± 1.5
N ₂ O emis.	7.33 ± 2.3	0.69 ± 0.27	0.33 ± 0.15
NH ₃ emis.	38.15 ± 20.8	2.45 ± 1.89	<0.01 ± <0.01
Total gaseous output	108.6 ± 50.09	22.29 ± 13.28	1.78 ± 1.98
DON leaching	0.01 ± <0.01	0.01 ± <0.01	0.01 ± <0.01
NO ₃ leaching	30.01 ± 29.9	1.46 ± 3.19	0.03 ± 0.04
Total leaching output	30.02 ± 29.9	1.47 ± 3.19	0.04 ± 0.04
N grain export	63.92 ± 5.17	0	0
N straw export	35.75 ± 2.67	29.77 ± 9.44	0
Total biomass output	99.67 ± 7.84	29.77 ± 9.44	0
Balance	-38.35 ± 87.83	-38.94 ± 25.91	5.20 ± 2.02

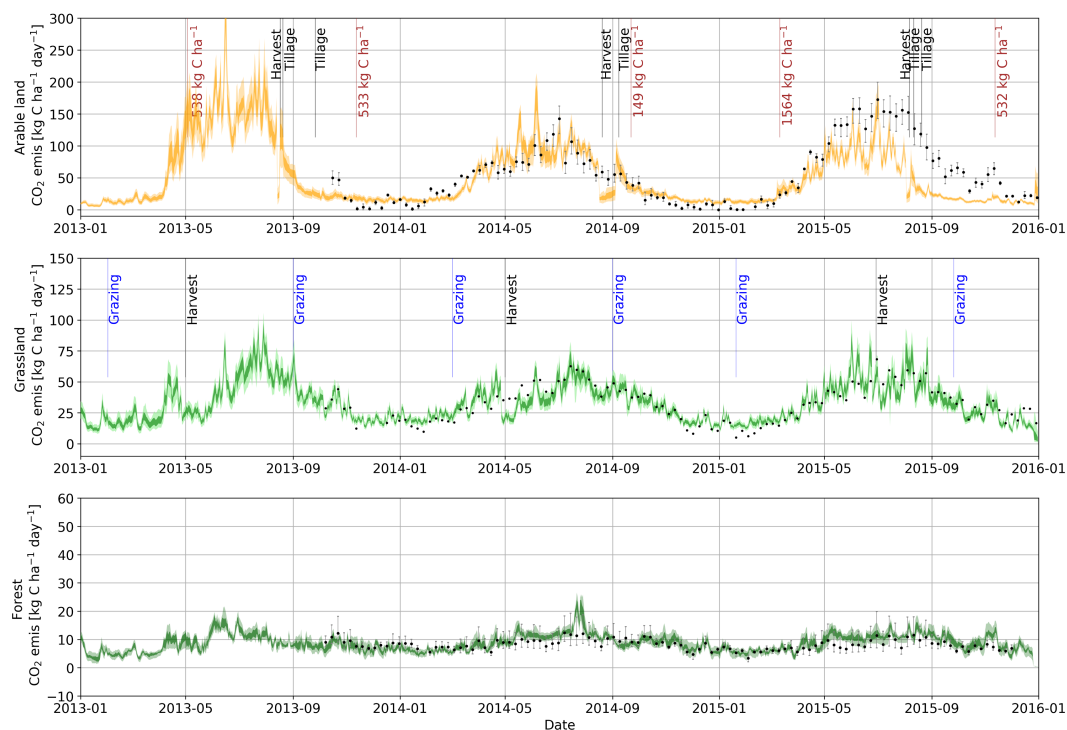


Figure 5. Modelled CO₂ emissions and management. Measurements are given as grey error bars showing the variance between the replicated transects and the mean value as a black dot. Posterior model uncertainty is given in light colour for the 5th and 95th percentiles and dark colour for the 25th and 75th percentiles. Vertical lines indicate management events. Brown coloured bars in the uppermost panel indicate manure application.

may contribute to the discrepancies between observed and modelled CO₂ emissions.

Grassland C cycle: the LandscapeDNDC simulations for the grassland system (G1) predict a mean annual gross car-

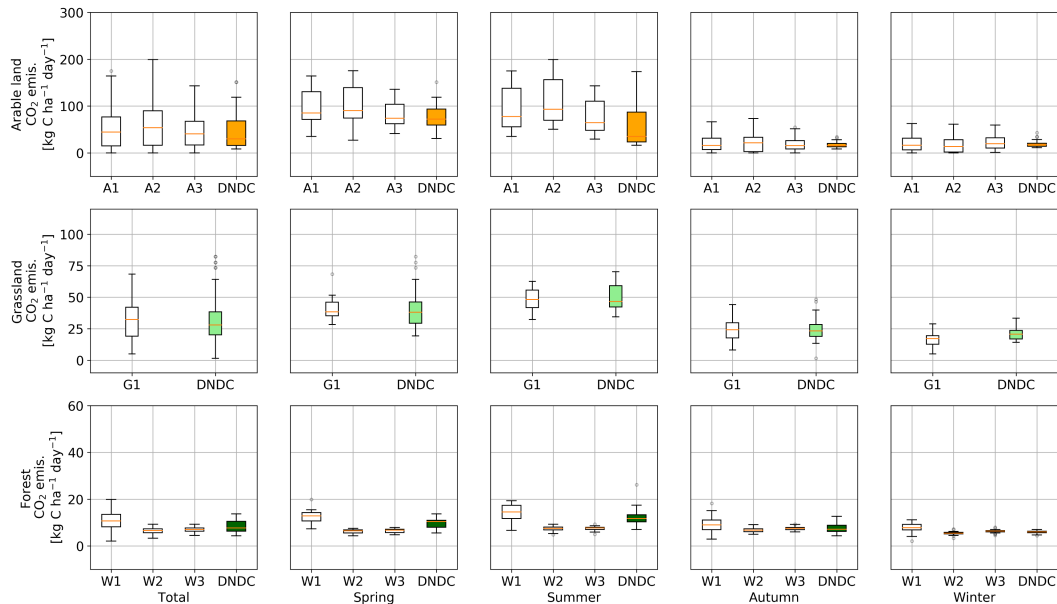


Figure 6. Observed and modelled CO₂ emissions for spring (21 March–20 June), summer (21 June–20 September), autumn (21 September–20 December), and winter (21 December–20 March).

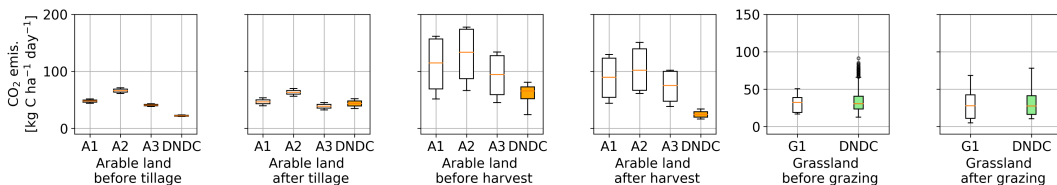


Figure 7. Management effects on CO₂ emissions. Measured and modelled emissions in a time window of 2 weeks before and 2 weeks after a management.

bon uptake of 16.9 ± 1.7 t C–CO₂ ha⁻¹ a⁻¹ and an annual loss of 13.2 ± 2.3 t C–CO₂ ha⁻¹ a⁻¹ through respiration. The rest is related to grazing ($0.2 \pm <0.01$ t C–CO₂ ha⁻¹ a⁻¹), harvesting (2.1 ± 0.7 t C–CO₂ ha⁻¹ a⁻¹) and allocation in the soil (1.4 ± 4.7 t C–CO₂ ha⁻¹ a⁻¹). The model cannot determine whether the system is net gaining or losing carbon. The annual mean and temporal dynamics of the modelled emissions are well in accordance with the measured emissions. The effect of grazing has a minor influence on the total ecosystem respiration (Fig. 7), resulting in a wider range of both measured and modelled emissions. Grazing, i.e. the reduction of root biomass, results in two contrary processes: a reduction in maintenance respiration and an increase in autotrophic respiration (Raich and Tufekciogul, 2000).

Forest C cycle: the forest model predicts an annual C input of 8.9 ± 0.6 t C–CO₂ ha⁻¹ a⁻¹, which is low compared to the estimations for old-growth beech forests in Europe, with reported rates from 14.4 to 18.3 t C–CO₂ ha⁻¹ a⁻¹ (Molina-Herrera et al., 2015). However, C uptake rates vary in magnitude, with values ranging from 3 to 34 t C–CO₂ ha⁻¹ a⁻¹ for different forests in different growing stages (Waring et al.,

1998). As our study site is a mixture of young and old beech trees, we assume that it has 40–50 % less biomass compared to an old beech forest. Of the modelled C input, 6.6 ± 0.5 t C–CO₂ ha⁻¹ a⁻¹ leaves the system as gaseous CO₂. The rest is accumulated in the biomass and soil. The annual mean and dynamics of the modelled emissions are in accordance with the measured emissions. We expected to see rising emissions with litter fall in autumn (Raich and Tufekciogul, 2000), but cannot report this effect, either with measurements or with model results (Fig. 6).

4 Conclusions

We presented a 2-year measurement campaign of trace gas emissions from adjacent land uses i.e. arable land, grassland and forest ecosystems, with concurrent model development and rigorous testing through a model–data fusion.

We found high emissions of N₂O and CO₂ on our arable land sites, low emissions on grassland sites and the lowest emissions on the forest sites. These observations enable us to investigate the underlying effects of plant growth, tem-

Table 5. Simulated carbon fluxes given by posterior model runs and their uncertainty on different land use in t C ha⁻¹ a⁻¹. C manure on grassland includes input by sheep's dung. Arable land model assumes 20 % return of stubble to field.

Modelled C flux	Arable land	Grassland	Forest
CO ₂ uptake	24.65 ± 1.32	16.8 ± 1.72	8.94 ± 0.56
C manure	1.06	0.07	0
Total input	25.71 ± 1.32	16.87 ± 1.72	8.94 ± 0.56
Growth respiration	2.53 ± 0.2	0.81 ± 0.27	1.44 ± 0.05
Heterotrophic respiration	4.69 ± 0.53	2.27 ± 0.9	2.04 ± 0.1
Maintenance respiration	13.31 ± 1.06	10.16 ± 1.13	3.11 ± 0.39
Total gaseous output	20.53 ± 1.79	13.24 ± 2.3	6.59 ± 0.54
DOC leaching	<0.01 ± <0.01	<0.01 ± <0.01	<0.01 ± <0.01
Total leaching output	<0.01	<0.01	<0.01
C bud export	1.97 ± 0.17	0	0
C straw export	2.75 ± 0.21	2.28 ± 0.72	0
Total biomass output	4.72 ± 0.38	2.28 ± 0.72	0
Balance	0.46 ± 3.49	1.35 ± 4.74	2.35 ± 1.1

Table 6. Overall posterior model performance of LandscapeDNDC on different land uses in reproducing GHG emission data. Subjectively classified into (1) good, (2) medium and (3) poor model performance in simulating reliable annual sums, seasonal patterns and magnitudes of management events (e.g. fertilizer application).

Modelled performance on each land use	N ₂ O emissions			CO ₂ emissions		
	annual	seasonal	management	annual	seasonal	management
Arable land (A1-3)	2	1	1	1	2	3
Grassland (G1)	1	2	1	1	1	1
Forest (W1-3)	2	2	n/a	1	2	n/a

n/a, not applicable, i.e. no forest management during modelled period from 2010 to 2016.

perature and WFPS, land use effects, seasonal patterns and management effects. Respiration amounts rise in less shaded (warmer) areas of the forest, while N₂O emissions increase towards the foothills of the forest and arable land sites due to nitrogen accumulation. Highly variable N₂O emissions in forests resulted in large uncertainties in the model verification data, which translated into large uncertainties in the model results for forests.

Detailed measured data on soil and management allowed us to fit the biogeochemical model LandscapeDNDC to the measured soil moisture, yield and GHG emissions of CO₂ and N₂O. A subjective conclusion about the overall model performance is shown in Table 6: The model reproduced the measured data reasonably well in time, separated into seasons and management events. The model performance was best in predicting management effects on N₂O emissions and annual CO₂ emissions for all land uses. With regard to land use, the simulations for grassland sites work best, followed by those for arable land. The simulations for N₂O emissions on arable land outperform those for CO₂, and vice versa for

grassland. Low emissions on forest sites were generally difficult to depict using our modelling approach.

The model–data fusion approach allowed us to identify model structural deficiencies that would likely increase model performances if addressed in LandscapeDNDC: missing N₂O uptake processes; missing NO₃⁻ (and potentially dissolved organic nitrogen) uptake through shallow groundwater; missing lateral interaction on hillslopes due to the 1-D model setup.

Furthermore, posterior model runs allowed for the quantification of the magnitude and uncertainty of unmeasured C and N cycle fluxes. The investigated forest site generally acts as the largest sink for C and N, with annual sequestration rates of 2.4 ± 1.1 t C ha⁻¹ and 5.2 ± 2.0 kg N ha⁻¹. Whether the extensive grazed grassland is also acting as a sink for C with 1.4 ± 4.7 t C ha⁻¹ per year remains uncertain, while the N cycle of the grassland model cannot be closed with the given settings. Shrinking N soil pools indicate a missing input, which we assume to be shallow groundwater with an additional N supply of approximately 38.9 ± 25.9 kg N ha⁻¹ a⁻¹.

Current land use in this catchment is dominated by forests (37 %) and arable land (35 %), whereas grassland sites (11 %) are mainly distributed along the stream. From the viewpoint of climate-smart landscapes, the measured data suggest the benefit of forests in a landscape, as they have the fewest GHG emissions. Riparian zones can act as sinks of N but only during the vegetation period and during times when roots have access to groundwater. Arable land use produces high amounts of N₂O, not throughout the year, but rather, in spring after fertilizer application.

The herein presented novel GHG study catchment enables a number of future studies. The forest sites could be further used to investigate the influence of leafs on the concentration of N through fall. The presented grassland dataset allows to quantify the nitrate uptake of riparian zones in more detail, e.g. by model coupling analysis, as done by Klatt et al. (2017), to account for potential interactions of land use patterns. Such a model setup would allow upscaling in space, e.g. for the generation of GHG inventories or an analysis of more detailed management scenarios in time. From the viewpoint of eutrophication and drinking water security, the presented agro-ecosystem plays a pivotal role, as it receives high amounts of reactive nitrogen (N) in the form of mineral fertilizer and manure. Our measured data can lead to novel understanding of how to develop and test mitigation measures to reduce N pollution on the landscape scale. The existing model setup can be further used in a forecast mode, e.g. to estimate optimal timing and location of fertilizer application to minimize N₂O emissions and NO₃⁻ leaching, while at least maintaining yields. Continuous measures of greenhouse gas emissions can be used to evaluate possible mitigation measures.

Code availability. The LandscapeDNDC framework is freely available upon request from <http://svn.imk-ifu.kit.edu/>. The SPOTPY tool, used for model–data fusion, is free and open source and is available from <https://pypi.python.org/pypi/spotpy>.

Data availability. All measured data are freely available upon request from <http://fb09-pasig.umwelt.uni-giessen.de:8081/>.

Appendix A

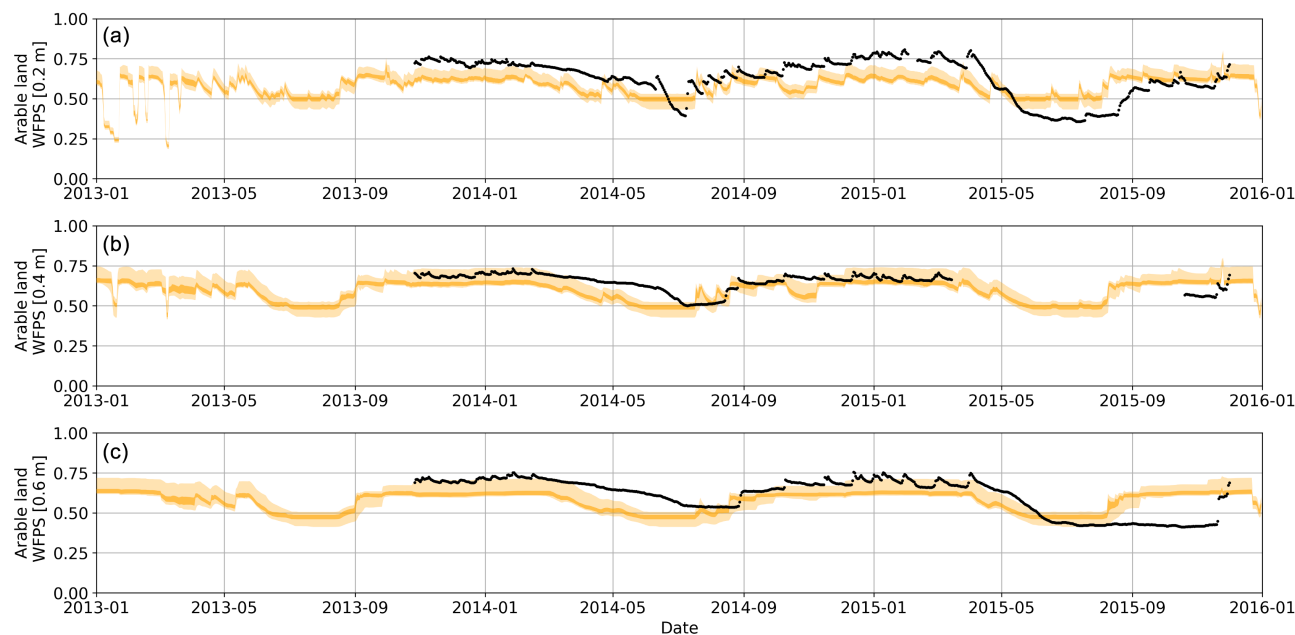


Figure A1. Modelled WFPS on arable land in different depths. RM-SEs ranging from 0.0774 to 0.1194 % WFPS (0.2 m), 0.0511 to 0.0955 % WFPS (0.4 m) and 0.0921 to 0.1193 % WFPS (0.6 m).

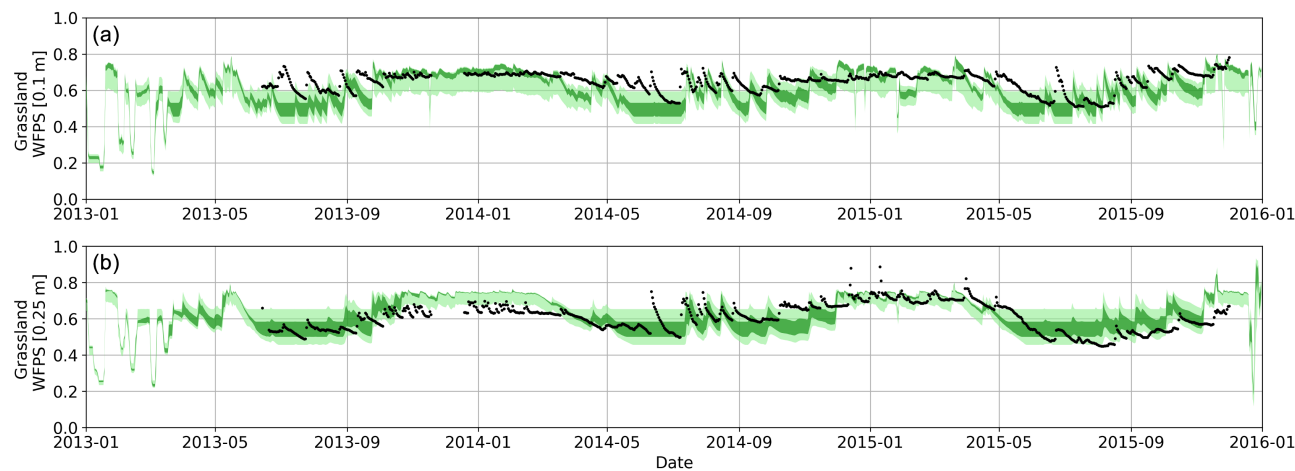


Figure A2. Modelled WFPS on grassland in different depths. RM-SEs ranging from 0.043 to 0.1481 % WFPS (0.1 m) and 0.056 to 0.1069 % WFPS (0.25 m).

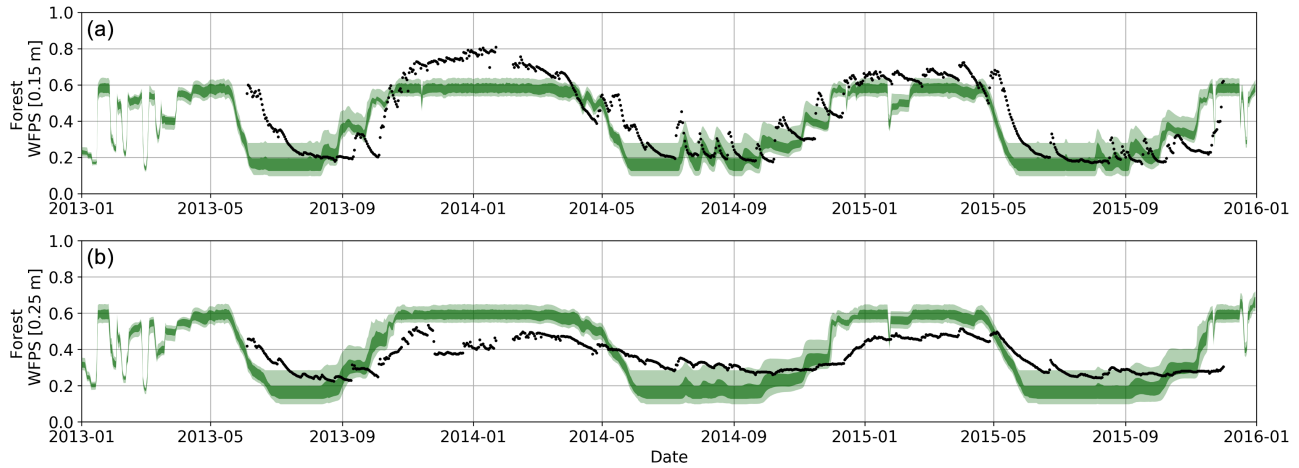


Figure A3. Modelled WFPS on forest in different depths. RMSEs ranging from 0.0817 to 0.1324 % WFPS (0.15 m) and 0.0812 to 0.1606 % WFPS (0.25 m).

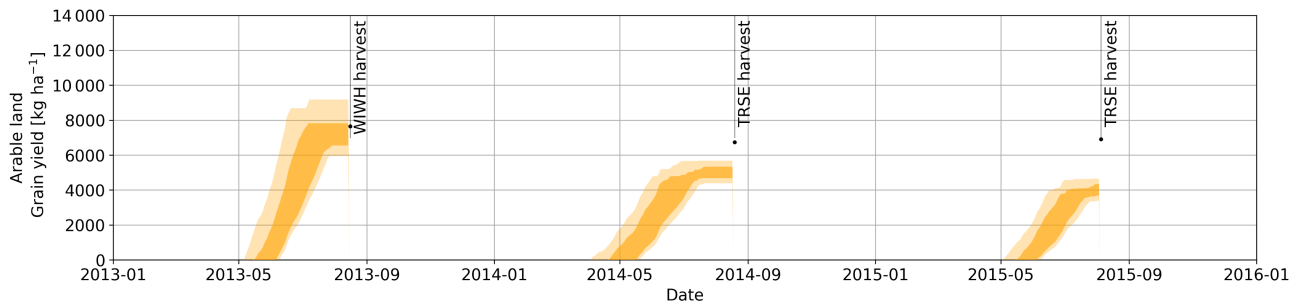


Figure A4. Modelled dry weight grain yield on arable land use. WIWH, winter wheat; TRSE, *Triticum secale*. RMSEs ranging from 1125.7 to 2529.2 kg ha⁻¹.

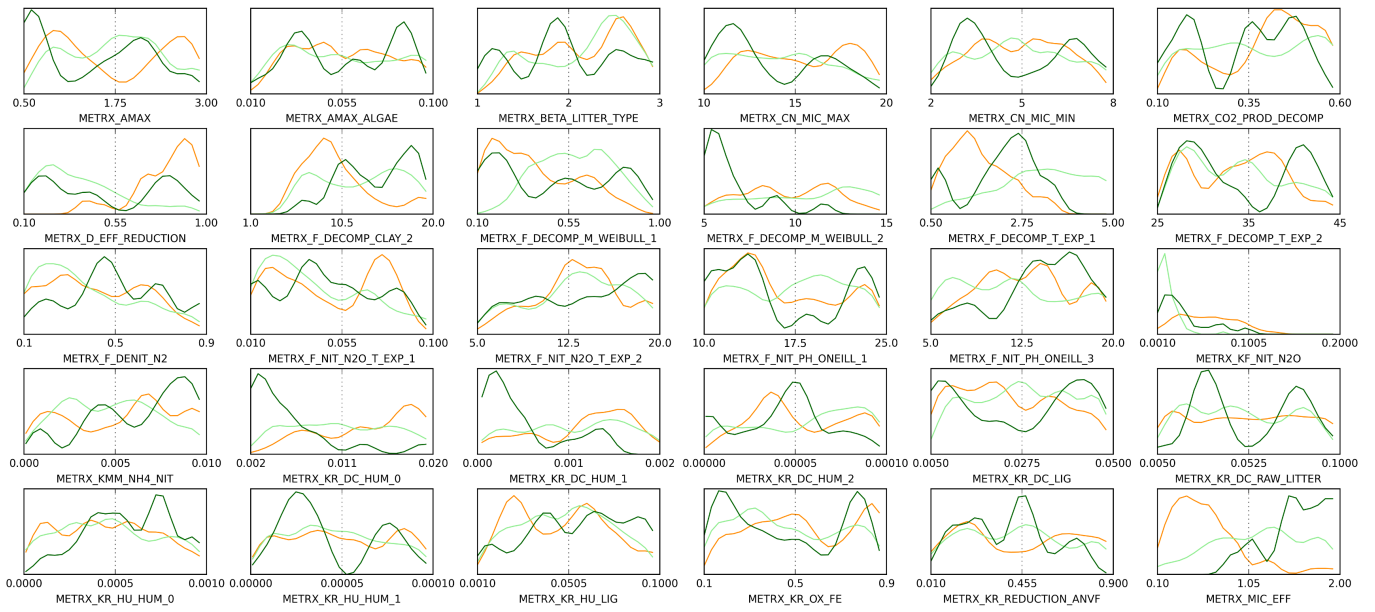


Figure A5. Posterior parameter distribution of the LandscapedNDC module MeTrx. Orange line, arable land; light green line, grassland; dark green line, forest model set-up.

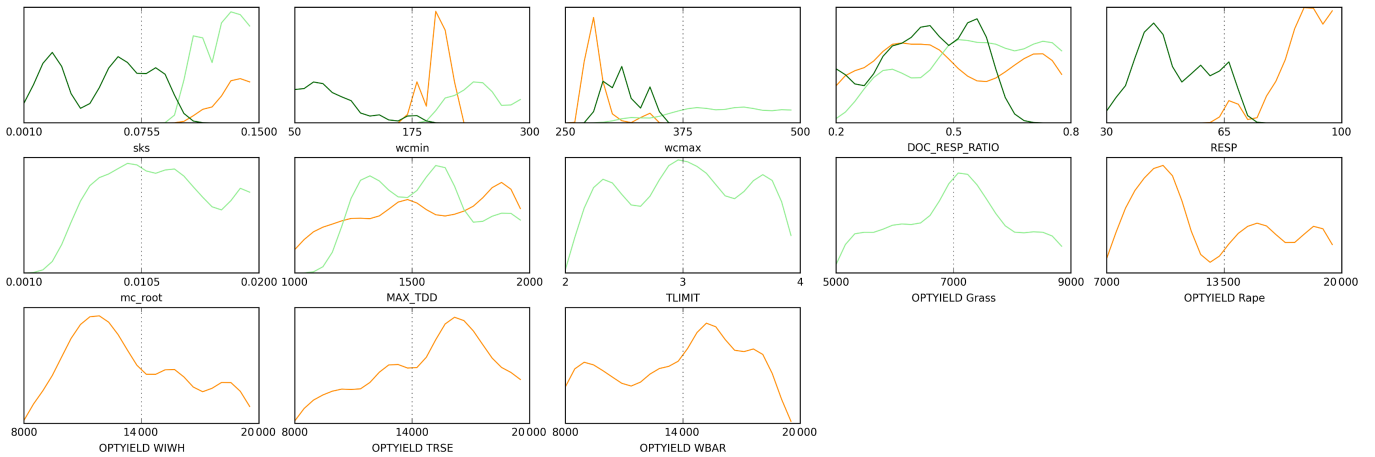


Figure A6. Posterior parameter distribution of the LandscapedNDC modules wcDNDC and physiology. Orange line, arable land; light green line, grassland; dark green line, forest model set-up.

Table A1. Input parameters for all investigated LandscapeDNDC modules with uniform distribution for Latin hypercube sampling. FASY, *Fagus sylvatica*; PERG, perennial grass.

Module	Parameter name	Description	Min	Max
wcDNDC	sk_s_arable	Value of soil layer for saturated hydraulic conductivity	0.1	0.2
wcDNDC	sk_s_grassland	Value of soil layer for saturated hydraulic conductivity	0.1	0.15
wcDNDC	sk_s_forest	Value of soil layer for saturated hydraulic conductivity	0.1	0.1
wcDNDC	wcmin_arable	Wilting point of soil layer	170	220
wcDNDC	wcmin_grassland	Wilting point of soil layer	200	300
wcDNDC	wcmin_forest	Wilting point of soil layer	40	200
wcDNDC	wcmax_arable	Field capacity of uppermost soil layer	270	350
wcDNDC	wcmax_grassland	Field capacity of soil layer	300	500
wcDNDC	wcmax_forest	Field capacity of soil layer	270	350
physiology	DOC_RESP_RATIO_FASY	Ratio of root exudates related to root growth respiration	0.1	0.6
physiology	RESP_FASY	Factor determining plant respiration	30	70
physiology	DOC_RESP_RATIO_PERG	Ratio of root exudates related to root growth respiration	0.2	0.8
physiology	MC_ROOT_PERG	Maintenance respiration coefficient of roots	0.001	0.02
physiology	MAX_TDD_PERG	Temperature degree days for full plant development	1200	2000
physiology	OPTYIELD_PERG	Optimum yield of crops and grasses	5000	9000
physiology	TLIMIT_PERG	Temperature limit for plant growth	2	4
physiology	DOC_RESP_RATIO_arable	Ratio of root exudates related to root growth respiration	0.2	0.8
physiology	MAX_TDD_arable	Temperature degree days for full plant development	1000	2000
physiology	RESP_arable	Factor determining plant respiration	30	100
physiology	OPTYIELD_rape	Optimum yield of rape	7000	20000
physiology	OPTYIELD_WIWH	Optimum yield of winter wheat	8000	20000
physiology	OPTYIELD_TRSE	Optimum yield of <i>Triticale</i>	8000	20000
physiology	OPTYIELD_WBAR	Optimum yield of winter barley	8000	20000
physiology	METRX_AMAX	Maximum microbial death rate	0.5	3
METRX	METRX_AMAX_ALGAE	Maximum decay rate of alga	0.01	0.1
METRX	METRX_BETA_LITTER_TYPE	Exp. fac. of litter decomposition red. depend. on lignin conc	1	3
METRX	METRX_CN_MIC_MAX	Maximum allowed C / N ratio for microbes	10	20
METRX	METRX_CN_MIC_MIN	Minimum allowed C / N ratio for microbes	2	8
METRX	METRX_CO2_PROD_DECOMP	Instantaneously production of CO ₂ during decomposition	0.1	0.6
METRX	METRX_D_EFF_REDUCTION	Reduction factor for gas diffusion	0.1	1
METRX	METRX_F_DECOMP_CLAY_2	Factor for clay dependency of decomposition	1	20
METRX	METRX_F_DECOMP_M_WEIBULL_1	Factor for water filled pore space dependency of decomposition	0.1	1
METRX	METRX_F_DECOMP_M_WEIBULL_2	Factor for water filled pore space dependency of decomposition	5	15
METRX	METRX_F_DECOMP_T_EXP_1	Factor for temperature dependency of decomposition	0.5	5
METRX	METRX_F_DECOMP_T_EXP_2	Factor for temperature dependency of decomposition	25	45
METRX	METRX_F_DENIT_N2	Factor determining amount denitrified nitrogen goes to N ₂	0.1	0.9
METRX	METRX_F_NIT_N2O_T_EXP_1	Factor for temp. depend. of N ₂ O prod. during nitrification	0.01	0.1
METRX	METRX_F_NIT_N2O_T_EXP_2	Factor for temperature dependency of N ₂ O production	5	20
METRX	METRX_F_NIT_PH_ONCELL_1	Factor for pH dependency of nitrification	10	25
METRX	METRX_F_NIT_PH_ONCELL_3	Factor for pH dependency of nitrification	5	20

Table A1. Continued.

Module	Parameter name	Description	Min	Max
METRX	METRX_KF_NIT_N2O	Maximum fraction of nitrified NH ₄ that goes to N ₂ O	0.001	0.2
METRX	METRX_KMM_NH4_NIT	Michaelis–Menten const. for NH ₄ depend. of nitrification	0.00001	0.01
METRX	METRX_KR_DC_HUM_0	Decomposition constant of recalcitrant young humus	0.002	0.02
METRX	METRX_KR_DC_HUM_1	Decomposition constant of recalcitrant old humus	0.00005	0.002
METRX	METRX_KR_DC_HUM_2	Decomposition constant of recalcitrant old humus	0.000001	0.0001
METRX	METRX_KR_DC_LIG	Decomposition constant of lignin	0.0005	0.05
METRX	METRX_KR_DC_RAW_LITTER	Decomposition constant of raw litter	0.005	0.1
METRX	METRX_KR_HU_HUM_0	Rate constant for humification of labile humus to recalcitrant young humus	0.000001	0.001
METRX	METRX_KR_HU_HUM_1	Rate constant for humification of recalcitrant young humus to recalcitrant old humus	0.000001	0.0001
METRX	METRX_KR_HU_LIG	Rate constant for humification of lignin	0.0001	0.1
METRX	METRX_KR_OX_FE	Rate constant of iron oxidation	0.1	0.9
METRX	METRX_KR_REDUCTION_ANVF	Decomposition reduction due anaerobicity	0.01	0.9
METRX	METRX_MIC_EFF	Microbial carbon use efficiency	0.1	2

Author contributions. TH, LB and RK designed and managed the experiments. DK and TH performed the simulations. TH prepared the paper with contributions from all co-authors.

Competing interests. The authors declare that they have no conflict of interest.

Acknowledgements. We acknowledge the financial support provided by the Deutsche Forschungsgemeinschaft (DFG) for Tobias Houska (BR2238/13-1). Special thanks go to Felix Kruck, Eva Holthof and Michael Herzog for their fieldwork during all weather conditions, Anja Schaefer-Schmid and Julia Valverde for lab analysis and providing the chamber sampling equipment, and the farmer for letting us study his land and providing the detailed management information.

Edited by: Sönke Zaehe

Reviewed by: two anonymous referees

References

- Arias-Navarro, C., Díaz-Pinés, E., Kiese, R., Rosenstock, T. S., Rufino, M. C., Stern, D., Neufeldt, H., Verchot, L. V., and Butterbach-Bahl, K.: Gas pooling: A sampling technique to overcome spatial heterogeneity of soil carbon dioxide and nitrous oxide fluxes, *Soil Biol. Biochem.*, 67, 20–23, <https://doi.org/10.1016/j.soilbio.2013.08.011>, 2013.
- Barton, L., Kiese, R., Gatter, D., Butterbach-Bahl, K., Buck, R., Hinz, C., and Murphy, D. V.: Nitrous oxide emissions from a cropped soil in a semi-arid climate, *Glob. Change Biol.*, 14, 177–192, <https://doi.org/10.1111/j.1365-2486.2007.01474.x>, 2008.
- Beven, K. and Binley, A.: The future of distributed models: Model calibration and uncertainty prediction, *Hydrol. Proc.*, 6, 279–298, <https://doi.org/10.1002/hyp.3360060305>, 1992.
- Bloom, A. A. and Williams, M.: Constraining ecosystem carbon dynamics in a data-limited world: integrating ecological “common sense” in a model-data fusion framework, *Biogeosciences*, 12, 1299–1315, <https://doi.org/10.5194/bg-12-1299-2015>, 2015.
- Boden, T. A., Marland, G., and Andres, R. J.: Global, regional and national fossil fuel CO₂ emissions, available from: http://cdiac.ornl.gov/trends/emis/overview_2007.html (last accessed: 17 August 2016), 2010.
- Bouwman, A. F., Boumans, L. J. M., and Batjes, N. H.: Emissions of N₂O and NO from fertilized fields: Summary of available measurement data, *Global Biogeochem. Cy.*, 16, 1–13, <https://doi.org/10.1029/2001GB001811>, 2002.
- Bremner, J. M.: Sources of nitrous oxide in soils, *Nutr. Cycl. Agroecosys.*, 49, 7–16, 1997.
- Burton, D. L., Li, X., and Grant, C. A.: Influence of fertilizer nitrogen source and management practice on N₂O emissions from two Black Chernozemic soils, *Can. J. Soil Sci.*, 88, 219–227, <https://doi.org/10.4141/CJSS06020>, 2008.
- Butterbach-Bahl, K., Baggs, E. M., Dannenmann, M., Kiese, R., and Zechmeister-Boltenstern, S.: Nitrous oxide emissions from soils: how well do we understand the processes and their controls?, *Philos. T. R. Soc. B*, 368, 20130122, <https://doi.org/10.1098/rstb.2013.0122>, 2013.
- Buyanovsky, G. A., Wagner, G. H., and Gantzer, C. J.: Soil respiration in a winter wheat ecosystem, *Soil Sci. Soc. Am. J.*, 50, 338–344, 1986.
- Cole, C. V., Duxbury, J., Freney, J., Heinemeyer, O., Minami, K., Mosier, A., Paustian, K., Rosenberg, N., Sampson, N., and Sauerbeck, D.: Global estimates of potential mitigation of greenhouse gas emissions by agriculture, *Nutr. Cycl. Agroecosys.*, 49, 221–228, <https://doi.org/10.1023/A:1009731711346>, 1997.
- Davidson, E. A.: Sources of nitric oxide and nitrous oxide following wetting of dry soil, *Soil Sci. Soc. Am. J.*, 56, 95–102, 1992.
- De Bruijn, A. M. G., Butterbach-Bahl, K., Blagodatsky, S., and Grote, R.: Model evaluation of different mechanisms driving freeze–thaw N₂O emissions, *Agr. Ecosyst. Environ.*, 133, 196–207, <https://doi.org/10.1016/j.agee.2009.04.023>, 2009.
- Demyan, M. S., Ingwersen, J., Funkuin, Y. N., Ali, R. S., Mirzaeitalarposhti, R., Rasche, F., Poll, C., Müller, T., Streck, T., and Kandeler, E.: Partitioning of ecosystem respiration in winter wheat and silage maize—modeling seasonal temperature effects, *Agric. Ecosyst. Environ.*, 224, 131–144, <https://doi.org/10.1016/j.agee.2016.03.039>, 2016.
- Flechard, C. R., Neftel, A., Jocher, M., Ammann, C., and Fuhrer, J.: Bi-directional soil/atmosphere N₂O exchange over two mown grassland systems with contrasting management practices, *Glob. Change Biol.*, 11, 2114–2127, <https://doi.org/10.1111/j.1365-2486.2005.01056.x>, 2005.
- Flechard, C. R., Nemitz, E., Smith, R. I., Fowler, D., Vermeulen, A. T., Bleeker, A., Erisman, J. W., Simpson, D., Zhang, L., and Tang, Y. S.: Dry deposition of reactive nitrogen to European ecosystems: a comparison of inferential models across the NitroEurope network, *Atmos. Chem. Phys.*, 11, 2703–2728, <https://doi.org/10.5194/acp-11-2703-2011>, 2011.
- Gabrielle, B., Laville, P., Duval, O., Nicoulaud, B., Geron, J.-C., and Hénault, C.: Process-based modeling of nitrous oxide emissions from wheat-cropped soils at the subregional scale, *Global Biogeochem. Cy.*, 20, GB4018, <https://doi.org/10.1029/2006GB002686>, 2006.
- Gilmanov, T. G., Soussana, J. F., Aires, L., Allard, V., Ammann, C., Balzarolo, M., Barcza, Z., Bernhofer, C., Campbell, C. L., and Cernusca, A.: Partitioning European grassland net ecosystem CO₂ exchange into gross primary productivity and ecosystem respiration using light response function analysis, *Agr. Ecosyst. Environ.*, 121, 93–120, <https://doi.org/10.1016/j.agee.2006.12.008>, 2007.
- Giltrap, D. L., Li, C., and Sagar, S.: DNDC: A process-based model of greenhouse gas fluxes from agricultural soils, *Agr. Ecosyst. Environ.*, 136, 292–300, <https://doi.org/10.1016/j.agee.2009.06.014>, 2010.
- Glatzel, S. and Stahr, K.: Methane and nitrous oxide exchange in differently fertilised grassland in southern Germany, *Plant Soil*, 231, 21–35, <https://doi.org/10.1023/A:1010315416866>, 2001.
- Graedel, T. E. and Crutzen, P. J.: The changing atmosphere, *Sci. Am.*, 58–68, 1989.
- Grote, R., Lehmann, E., Brümmer, C., Brüggemann, N., Szarzynski, J., and Kunstmann, H.: Modelling and observation of biosphere–atmosphere interactions in natural savannah in Burkina Faso, West Africa, *Phys. Chem. Earth Parts ABC*, 34, 251–260, <https://doi.org/10.1016/j.pce.2008.05.003>, 2009.

- Haas, E., Klatt, S., Fröhlich, A., Kraft, P., Werner, C., Kiese, R., Grote, R., Breuer, L., and Butterbach-Bahl, K.: LandscapeDNDC: a process model for simulation of biosphere–atmosphere–hydrosphere exchange processes at site and regional scale, *Landsc. Ecol. Eng.*, 28, 615–636, <https://doi.org/10.1007/s10980-012-9772-x>, 2013.
- Houska, T., Kraft, P., Chamorro-Chavez, A., and Breuer, L.: SPOTting Model Parameters Using a Ready-Made Python Package, *PLoS ONE*, 10, e0145180, <https://doi.org/10.1371/journal.pone.0145180>, 2015.
- Houska, T., Kraft, P., Liebermann, R., Klatt, S., Kraus, D., Haas, E., Santabárbara, I., Kiese, R., Butterbach-Bahl, K., Müller, C., and Breuer, L.: Rejecting hydro-biogeochemical model structures by multi-criteria evaluation, *Environ. Model. Softw.*, 93, 1–12, <https://doi.org/10.1016/j.envsoft.2017.03.005>, 2017.
- IPCC: Revised 1996 IPCC guidelines for national greenhouse gas inventories. v. 1: Greenhouse gas inventory reporting instructions.-v. 2: Greenhouse gas inventory workbook.-v. 3: Greenhouse gas inventory reference manual, 1997.
- IPCC: Contribution of working group III to the fourth assessment report of the intergovernmental panel on climate change, edited by: Metz, B., Davidson, O. R., Bosch, P. R., Dave, R., and Meyer, L. A., 2007.
- Janssens, I. A., Lankreijer, H., Matteucci, G., Kowalski, A. S., Buchmann, N., Epron, D., Pilegaard, K., Kutsch, W., Longdoz, B., and Grünwald, T.: Productivity overshadows temperature in determining soil and ecosystem respiration across European forests, *Glob. Change Biol.*, 7, 269–278, <https://doi.org/10.1046/j.1365-2486.2001.00412.x>, 2001.
- Jansson, P.-E.: CoupModel: model use, calibration, and validation, *Trans. ASABE*, 55, 1337–1344, <https://doi.org/10.13031/2013.42245>, 2012.
- Jungkunst, H. F., Freibauer, A., Neufeldt, H., and Bareth, G.: Nitrous oxide emissions from agricultural land use in Germany – a synthesis of available annual field data, *J. Plant Nutr. Soil Sci.*, 169, 341–351, <https://doi.org/10.1002/jpln.200521954>, 2006.
- Kammann, C., Grünhage, L., Müller, C., Jacobi, S., and Jäger, H.-J.: Seasonal variability and mitigation options for N₂O emissions from differently managed grasslands, *Environ. Pollut.*, 102, 179–186, [https://doi.org/10.1016/S0269-7491\(98\)80031-6](https://doi.org/10.1016/S0269-7491(98)80031-6), 1998.
- Kavetski, D., Kuczera, G., and Franks, S. W.: Bayesian analysis of input uncertainty in hydrological modeling: 1. Theory, *Water Resour. Res.*, 42, W03407, <https://doi.org/10.1029/2005WR004368>, 2006.
- Keenan, T. F., Carbone, M. S., Reichstein, M., and Richardson, A. D.: The model–data fusion pitfall: assuming certainty in an uncertain world, *Oecologia*, 167, 587, <https://doi.org/10.1007/s00442-011-2106-x>, 2011.
- Kiese, R., Heinzeller, C., Werner, C., Wochele, S., Grote, R., and Butterbach-Bahl, K.: Quantification of nitrate leaching from German forest ecosystems by use of a process oriented biogeochemical model, *Environ. Pollut.*, 159, 3204–3214, <https://doi.org/10.1016/j.envpol.2011.05.004>, 2011.
- Kim, Y., Seo, Y., Kraus, D., Klatt, S., Haas, E., Tenhunen, J., and Kiese, R.: Estimation and mitigation of N₂O emission and nitrate leaching from intensive crop cultivation in the Haean catchment, South Korea, *Sci. Total Environ.*, 529, 40–53, <https://doi.org/10.1016/j.scitotenv.2015.04.098>, 2015.
- Klatt, S., Kraus, D., Kraft, P., Breuer, L., Wlotzka, M., Heuveline, V., Haas, E., Kiese, R., and Butterbach-Bahl, K.: Exploring impacts of vegetated buffer strips on nitrogen cycling using a spatially explicit hydro-biogeochemical modeling approach, *Environ. Model. Softw.*, 90, 55–67, <https://doi.org/10.1016/j.envsoft.2016.12.002>, 2017.
- Kraus, D., Weller, S., Klatt, S., Haas, E., Wassmann, R., Kiese, R., and Butterbach-Bahl, K.: A new LandscapeDNDC biogeochemical module to predict CH₄ and N₂O emissions from lowland rice and upland cropping systems, *Plant Soil*, 386, 125–149, <https://doi.org/10.1007/s11104-014-2255-x>, 2015.
- Li, C., Aber, J., Stange, F., Butterbach-Bahl, K., and Papen, H.: A process-oriented model of N₂O and NO emissions from forest soils: 1. Model development, *J. Geophys. Res.*, 105, 4369–4384, <https://doi.org/10.1029/1999JD900949>, 2000.
- Liebermann, R., Houska, T., Kraft, P., Klatt, S., Kraus, D., Haas, E., Müller, C., and Breuer, L.: Closing the N-budget: How Simulated Groundwater-borne Nitrate Supply Affects Plant Growth and Greenhouse Gas Emissions on a Temperate Grassland, *PLoS ONE*, submitted, 2017.
- Lohila, A., Aurela, M., Regina, K., and Laurila, T.: Soil and total ecosystem respiration in agricultural fields: effect of soil and crop type, *Plant Soil*, 251, 303–317, <https://doi.org/10.1023/A:1023004205844>, 2003.
- Molina-Herrera, S., Grote, R., Santabárbara-Ruiz, I., Kraus, D., Klatt, S., Haas, E., Kiese, R., and Butterbach-Bahl, K.: Simulation of CO₂ Fluxes in European Forest Ecosystems with the Coupled Soil-Vegetation Process Model “LandscapeDNDC”, *Forests*, 6, 1779–1809, <https://doi.org/10.3390/f6061779>, 2015.
- Molina-Herrera, S., Haas, E., Klatt, S., Kraus, D., Augustin, J., Magliulo, V., Tallec, T., Ceschia, E., Ammann, C., and Loubet, B.: A modeling study on mitigation of N₂O emissions and NO₃ leaching at different agricultural sites across Europe using LandscapeDNDC, *Sci. Total Environ.*, 553, 128–140, <https://doi.org/10.1016/j.scitotenv.2015.12.099>, 2016.
- Myhre, G., Shindell, D., Bréon, F.-M., Collins, W., Fuglestvedt, J., Huang, J., Koch, D., Lamarque, J.-F., Lee, D., and Mendoza, B.: Anthropogenic and natural radiative forcing, *IPCC WGI Fifth Assess. Rep.*, 423, 658–740, 2013.
- Nefel, A., Flechard, C., Ammann, C., Conen, F., Emmenegger, L., and Zeyer, K.: Experimental assessment of N₂O background fluxes in grassland systems, *Tellus B*, 59, 470–482, <https://doi.org/10.1111/j.1600-0889.2007.00273.x>, 2007.
- Oenema, O., Velthof, G. L., Yamulki, S., and Jarvis, S. C.: Nitrous oxide emissions from grazed grassland, *Soil Use Manag.*, 13, 288–295, <https://doi.org/10.1111/j.1475-2743.1997>, 1997.
- Oijen, M. V., Rougier, J., and Smith, R.: Bayesian calibration of process-based forest models: bridging the gap between models and data, *Tree Physiol.*, 25, 915–927, <https://doi.org/10.1093/treephys/25.7.915>, 2005.
- Papen, H. and Butterbach-Bahl, K.: A 3-year continuous record of nitrogen trace gas fluxes from untreated and limed soil of a N-saturated spruce and beech forest ecosystem in Germany: 1. N₂O emissions, *J. Geophys. Res.-Atmos.*, 104, 18487–18503, <https://doi.org/10.1029/1999JD900293>, 1999.
- Parton, W. J., Hartman, M., Ojima, D., and Schimel, D.: DAYCENT and its land surface submodel: description and testing, *Glob. Planet. Change*, 19, 35–48, [https://doi.org/10.1016/S0921-8181\(98\)00040-X](https://doi.org/10.1016/S0921-8181(98)00040-X), 1998.

- Raich, J. W. and Schlesinger, W. H.: The global carbon dioxide flux in soil respiration and its relationship to vegetation and climate, *Tellus B*, 44, 81–99, <https://doi.org/10.1034/j.1600-0889.1992>.
- Raich, J. W. and Tufekciogul, A.: Vegetation and soil respiration: correlations and controls, *Biogeochemistry*, 48, 71–90, <https://doi.org/10.1023/A:1006112000616>, 2000.
- Ravishankara, A. R., Daniel, J. S., and Portmann, R. W.: Nitrous oxide (N₂O): the dominant ozone-depleting substance emitted in the 21st century, *Science*, 326, 123–125, <https://doi.org/10.1126/science.1176985>, 2009.
- Rochette, P., Flanagan, L. B., and Gregorich, E. G.: Separating soil respiration into plant and soil components using analyses of the natural abundance of carbon-13, *Soil Sci. Soc. Am. J.*, 63, 1207–1213, 1999.
- Savage, K., Phillips, R., and Davidson, E.: High temporal frequency measurements of greenhouse gas emissions from soils, *Biogeosciences*, 11, 2709–2720, <https://doi.org/10.5194/bg-11-2709-2014>, 2014.
- Seifert, A.-G., Roth, V.-N., Dittmar, T., Gleixner, G., Breuer, L., Houska, T., and Marxsen, J.: Comparing molecular composition of dissolved organic matter in soil and stream water: Influence of land use and chemical characteristics, *Sci. Total Environ.*, 571, 142–152, <https://doi.org/10.1016/j.scitotenv.2016.07.033>, 2016.
- Siemens, J. and Kaupenjohann, M.: Contribution of dissolved organic nitrogen to N leaching from four German agricultural soils, *J. Plant Nutr. Soil Sci.*, 165, 675–681, <https://doi.org/10.1002/jpln.200290002>, 2002.
- Smith, K. A., Ball, T., Conen, F., Dobbie, K. E., Massheder, J., and Rey, A.: Exchange of greenhouse gases between soil and atmosphere: interactions of soil physical factors and biological processes, *Eur. J. Soil Sci.*, 54, 779–791, <https://doi.org/10.1046/j.1351-0754.2003.0567.x>, 2003.
- Subke, J.-A., Reichstein, M., and Tenhunen, J. D.: Explaining temporal variation in soil CO₂ efflux in a mature spruce forest in Southern Germany, *Soil Biol. Biochem.*, 35, 1467–1483, [https://doi.org/10.1016/S0038-0717\(03\)00241-4](https://doi.org/10.1016/S0038-0717(03)00241-4), 2003.
- Suleau, M., Moureaux, C., Dufranne, D., Buysse, P., Bodson, B., Destain, J.-P., Heinesch, B., Debacq, A., and Aubinet, M.: Respiration of three Belgian crops: partitioning of total ecosystem respiration in its heterotrophic, above-and below-ground autotrophic components, *Agr. Forest Meteorol.*, 151, 633–643, <https://doi.org/10.1016/j.agrformet.2011.01.012>, 2011.
- Thorntwaite, C. W., Mather, J. R.: Instructions and tables for computing potential evapotranspiration and the water balance, *Publ. Climatol.*, 10, 185–311, 1957.
- Vrugt, J. A.: Markov chain Monte Carlo simulation using the DREAM software package: Theory, concepts, and MATLAB implementation, *Environ. Model. Softw.*, 75, 273–316, <https://doi.org/10.1016/j.envsoft.2015.08.013>, 2016.
- Wang, G. and Chen, S.: A review on parameterization and uncertainty in modeling greenhouse gas emissions from soil, *Geoderma*, 170, 206–216, <https://doi.org/10.1016/j.geoderma.2011.11.009>, 2012.
- Wang, Y.-P., Trudinger, C. M., and Enting, I. G.: A review of applications of model–data fusion to studies of terrestrial carbon fluxes at different scales, *Agr. Forest Meteorol.*, 149, 1829–1842, <https://doi.org/10.1016/j.agrformet.2009.07.009>, 2009.
- Waring, R. H., Landsberg, J. J., and Williams, M.: Net primary production of forests: a constant fraction of gross primary production?, *Tree Physiol.*, 18, 129–134, <https://doi.org/10.1093/treephys/18.2.129>, 1998.
- Wlotzka, M., Haas, E., Kraft, P., Heuveline, V., Klatt, S., Kraus, D., Butterbach-Bahl, K., and Breuer, L.: Dynamic Simulation of Land Management Effects on Soil N₂O Emissions using a coupled Hydrology-Ecosystem Model, *Preprint Series of the Engineering Mathematics and Computing Lab*, 3, 1–20, <https://doi.org/10.11588/emclpp.2013.03.11824>, 2013.
- Wohlfahrt, G., Bahn, M., Haslwanter, A., Newesely, C., and Cernusca, A.: Estimation of daytime ecosystem respiration to determine gross primary production of a mountain meadow, *Agr. Forest Meteorol.*, 130, 13–25, <https://doi.org/10.1016/j.agrformet.2005.02.001>, 2005a.
- Wohlfahrt, G., Anfang, C., Bahn, M., Haslwanter, A., Newesely, C., Schmitt, M., Drösler, M., Pfadenhauer, J., and Cernusca, A.: Quantifying nighttime ecosystem respiration of a meadow using eddy covariance, chambers and modelling, *Agr. Forest Meteorol.*, 128, 141–162, <https://doi.org/10.1016/j.agrformet.2004.11.003>, 2005b.
- Xiang, S.-R., Doyle, A., Holden, P. A., and Schimel, J. P.: Drying and rewetting effects on C and N mineralization and microbial activity in surface and subsurface California grassland soils, *Soil Biol. Biochem.*, 40, 2281–2289, <https://doi.org/10.1016/j.soilbio.2008.05.004>, 2008.